

We measure  $dT_0/dP \sim -5$  K/kbar.

Barrett's model predicts the correct sign for  $d \ln T_1/dP$ . As the volume is decreased, the nearest neighbors of the ion would confine it to a smaller volume, thus raising the energy of the lowest quantum level, and hence  $T_1$ . However, as pointed out above, either the measured value of  $d \ln T_1/dP$  is too large, or that for  $|dT_0/dP|$  is too small, to be consistent with Eq. (8). Since  $dT_0/dP$  is similar

to that measured for other perovskites, one might conclude that  $d \ln T_1/dP$  is anomalous and that  $T_1$  is not understood theoretically. Clearly more theoretical work is required.

#### ACKNOWLEDGMENTS

I would like to thank G. A. Samara for suggesting this problem. Steve Peerman and Gary Clendenen deserve much credit for making the measurements.

†Work supported by the U.S. AEC.

<sup>1</sup>J. K. Hulm, Proc. Phys. Soc. (London) **A63**, 1184 (1950).

<sup>2</sup>J. K. Hulm, B. T. Matthias, and E. A. Long, Phys. Rev. **79**, 885 (1949).

<sup>3</sup>J. C. Slater, Phys. Rev. **78**, 748 (1950).

<sup>4</sup>J. H. Barrett, Phys. Rev. **86**, 118 (1952).

<sup>5</sup>G. A. Samara, in *Advances in High Pressure Research*, edited by R. S. Bradley (Academic, New York, 1969), Vol. 3, Chap. 3.

<sup>6</sup>T. Sakudo and H. Unoki, Phys. Rev. Letters **26**, 851 (1971).

<sup>7</sup>Obtained from Electro-Optical Division, Sanders Assoc., 95 Canal, Nashua, N. H.

<sup>8</sup>D. N. Lyon, D. B. McWhan, and A. L. Stevens, Rev. Sci. Instr. **38**, 1234 (1967).

<sup>9</sup>J. E. Schirber, Cryogenics **10**, 418 (1970). The apparatus used was constructed by L. R. Edwards of this laboratory.

<sup>10</sup>J. S. Dugdale, Nuovo Cimento Suppl. **9**, 27 (1958).

<sup>11</sup>S. H. Wemple, Phys. Rev. **137**, A1575 (1965).

<sup>12</sup>S. H. Wemple, A. Jayaraman, and M. DiDomenico, Jr., Phys. Rev. Letters **17**, 142 (1966).

<sup>13</sup>G. Shirane, R. Nathans, and V. J. Minkiewicz, Phys. Rev. **157**, 396 (1967).

<sup>14</sup>R. A. Cowley, Phil. Mag. **11**, 673 (1965).

<sup>15</sup>N. S. Gillis and T. R. Koehler Phys. Rev. B (to be published).

## Electronic Defect Structure of Single-Crystal ThO<sub>2</sub> by Thermoluminescence

Elward T. Rodine\*

*Systems Research Laboratories, Inc., Dayton, Ohio 45440*

and

Peter L. Land

*Aerospace Research Laboratories, Wright-Patterson AFB, Ohio 45433*

(Received 18 January 1971)

Some electronic defects and the associated photoelectronic processes in ThO<sub>2</sub> are analyzed by utilizing the data from thermoluminescence (TL) and EPR measurements on a number of rare-earth-doped and undoped single crystals from various sources. (The EPR measurements were made by others.) Some fluorescence and absorption measurements are also utilized. Some TL glow peaks in the undoped ThO<sub>2</sub> correlate with the annealing of EPR spectra which are associated with trapped electrons. The similarity of glow curves for different crystals, the lack of hyperfine EPR structure, and the dependence on rare-earth doping suggests that some of the major electron traps are associated with oxygen vacancies, which may be complexed. The TL and EPR were induced by uv excitation, which created electrons and holes which are trapped. Some of the hole traps are identified as rare-earth ions in cubic sites. The rare earths provide all of the TL and fluorescence observed in Li<sub>2</sub>O · 2WO<sub>3</sub> flux-grown ThO<sub>2</sub>, and the total TL at saturation depends on the doping level. The TL excitation spectra and optical absorption measurements on Li<sub>2</sub>O · 2WO<sub>3</sub> flux-grown undoped thoria indicate a band gap of 5.75 eV which is larger than previously reported. The thermal activation energies are given for electron traps, and some indications of relative cross sections for electron or hole trapping or recombination processes are reported.

### INTRODUCTION

We have measured the thermoluminescence (TL) from a large number of ThO<sub>2</sub> single crystals. The crystals represent several different methods of

growth and have a wide variation of impurity content that includes intentional rare-earth doping. This paper deals primarily with the results and conclusions derived from the measurements on one group of crystals. More detailed data on these

crystals and on the crystals from other sources, and a more extensive discussion of the experimental procedures are contained in a doctoral dissertation<sup>1</sup> and an interim technical report.<sup>2</sup> The emphasized group of crystals was also studied by electron paramagnetic resonance (EPR) and the detailed data and analysis which we draw on are contained in a technical report by Neaves and Tint,<sup>3</sup> in a doctoral dissertation by Tint,<sup>4</sup> and, to a lesser extent, in interim technical reports by Wagner, Feldman, and Murphy.<sup>5</sup>

The intent of this investigation was to characterize some of the electronic defect structure of thoria by studying the TL and some other related optical properties, and if possible to identify the associated ionic defect structure. We therefore made a rather thorough study of the nature of the TL emission and of the effects of varying the excitation parameters. The EPR studies mentioned above are part of a cooperative, although independent, effort and we have therefore used the data and analysis of those groups in making a rather detailed interpretation of the processes.

The TL of thoria is bright when the crystals contain even trace amounts of rare-earth ions and no poisons; the peaks are well separated, and there are a relatively small number of major peaks in the range 77–600 °K which are common to many crystals. The primary excitation of TL is across the band gap in the high-purity and rare-earth-doped thoria.

The simple crystal structure (fluorite) and the relatively recent availability of high-quality single crystals which were generously supplied by Finch and Clark contributed to the selection of thoria for this study of defect structure by means of thermoluminescence. Previous investigations of the TL of ThO<sub>2</sub> are much less extensive. Greener *et al.*<sup>6</sup> examined the TL of some powdered thoria after room-temperature irradiation with <sup>60</sup>Co  $\gamma$  rays. Finch *et al.*<sup>7</sup> studied the TL of some thoria crystals, that were relatives to those supplied to us, after room-temperature excitation. Linares also reported some TL measurements on crystals that he grew.<sup>8</sup>

In this paper the experimental results and analysis for various measurements are presented in the following order: (a) sample description and nomenclature, (b) glow curves for various crystals, (c) TL intensity versus uv dose, (d) energy and frequency-factor analysis, (e) emission spectra for TL and fluorescence, (f) TL excitation spectra and optical absorption, (g) bleaching of TL, (h) electron paramagnetic resonance, and (i) effects of impurities. Finally we discuss the intrinsic-defect models which have been considered in attempting to explain the observations. Some are shown to be inappropriate to the data while others require

further consideration.

#### EQUIPMENT

The experimental apparatus used in this investigation was described in detail by Land and Wysong.<sup>9</sup> The central piece of apparatus was a rotatable variable-temperature optical cryochamber which was mounted on a heavy optical bench for convenience; it permitted us to irradiate the sample at liquid-nitrogen temperature through one quartz window, rotate the sample and cold finger 180 degrees, and measure the emission through the opposite window while warming. A third window was used for visual inspection or bleaching and a port on the fourth side led to the vacuum system. Excitation and emission apparatus could be connected to the ports in a light-tight manner.

The heater was a platinum wire-wound resistance heater which was imbedded in the copper sample block. A circuit consisting of resistors and thermistors was used to attain a reasonably linear heating rate from liquid-nitrogen temperature to 100 °C. The heating rate over most of the temperature range was about 30 °C/min although by 300 °C the heating rate dropped to 15 °C/min.

The most frequently used uv source was a Sylvania DE50 deuterium lamp operated at 32 W. This lamp is one of the sources available for the Bausch and Lomb high-intensity grating monochromator. For high excitation the deuterium lamp was used without the monochromator, in which case the light was focused by a quartz lens and provided an intensity of about 13 mW/cm<sup>2</sup>.

The basic emission detector was an RCA-1P28 photomultiplier, operated at 1000 V. When greater sensitivity (especially in the red) was required, an EMI-9558Q photomultiplier was used. The current in the photomultiplier was measured by a Keithley electrometer. The 0–1-V output of the electrometer was recorded on a Varian G-14 strip-chart recorder. The thermocouple voltage was reduced to a 0–1-mV range by a potentiometer and recorded on an identical recorder. An event marker permitted synchronization of the temperature and photomultiplier response records.

The emission spectra in most cases were measured with a rotating filter wheel.<sup>9</sup> The filter wheel held eight Optics Technology interference filters and was mounted between the sample and the photomultiplier in a light-tight manner and rotated at an appropriate speed as the sample was heated. The application of suitable normalization factors for the relative transmission of the filters, the response of the photomultiplier, etc., permitted us to obtain low-resolution emission analyses at any temperature from the simultaneous glow curves which were generated.

In cases where line spectra were present, we mounted the monochromator between the sample and photomultiplier and manually scanned as the sample was heated. Selected regions of the spectrum were also scanned with a SPEX 1700 spectrometer for higher resolution.

The light sources, monochromators, and photomultipliers were calibrated with a Hilger-Watts thermopile, used in conjunction with a light chopper and phase-lock amplifier.

Prior to mounting, the samples were washed in HCl to remove flux residue and then in  $\text{NH}_4\text{OH}$ . They were rinsed in distilled water in an ultrasonic cleaner and inspected for cleanliness under a microscope.

The samples were mounted on the copper sample block with Sauereisen Super Sealing Varnish No. 66. The varnish had sufficient mechanical strength and negligible TL over the temperature range utilized. In earlier studies of other materials we established that the temperature differences between the front and back of the samples were much less than the width of a typical TL peak and were therefore unimportant.<sup>10,11</sup>

## EXPERIMENTAL RESULTS

### Sample Description and Nomenclature

Table I describes some of the physical characteristics of the samples used. The first column gives the sample number of the principal crystal to be discussed and also the numbers of the other crystals from the same batch which have similar properties. Note that the numbering system specifies the source of the samples.

Most of the crystals used here were grown by Finch and Clark of ORNL from a lithium ditungstate solvent.<sup>12</sup> Batch No. 1 was grown undoped and provided a number of crystals that were studied extensively. The crystals could be classified into two groups by their TL as indicated in Table I. The principal crystals from this batch were OR1, OR2, OR7, and OR8.

Batch No. 2 was grown with the hope of doping the crystals with Ca, but only a small amount of Ca was incorporated. The crystals were similar in appearance to the original batch but the TL was much weaker and the peaks exceptionally well resolved. The eight batches of rare-earth-doped crystals each contained many crystals of various sizes; in some cases the largest crystals from a batch were smaller than  $10^{-3} \text{ cm}^3$ .

The other crystals were obtained as indicated in Table I. The arc-grown crystals obtained from the Franklin Institute were similar to the crystals used by Danforth.<sup>13</sup> The Perkin-Elmer crystals were grown by Linares from a lead flux.<sup>8</sup> The powder sample ESP-1 was formed by mixing some

high-purity powder with silicone vacuum grease; this was not a good technique because of the TL and absorption of the vacuum grease.

### Glow Curves for Various Crystals

Typical glow curves from some of the samples are shown in Figs. 1 and 2. Excitation conditions were similar in all cases and represent, in most cases, saturation conditions. The intensity scales have been adjusted so that the glow curves from very bright samples could be shown with those from the relatively weak samples. During a normal run, the electrometer scale is changed frequently so small peaks barely appearing in the composite curves can be studied in detail.

Most of the TL peaks are well separated and clean without a great deal of overlap and without the presence of many "shoulders." The peaks from PE2 are an exception to this. However, some of the peaks which appear pure and singular will be shown to be complex. For example, at high-dose levels one component may dominate, yielding the appearance of a singular peak.

Nearly all of the samples have major peaks between  $-120$  and  $-100^\circ\text{C}$  and between  $-20$  and  $-10^\circ\text{C}$ . There are exceptions to this, i. e., the  $\text{ThO}_2:\text{Eu}$  sample has a major peak at  $-135^\circ\text{C}$  and OR4 has a peak at  $-95^\circ\text{C}$  as well as at  $-120^\circ\text{C}$ . Smaller peaks at  $-160$  and  $-70^\circ\text{C}$  are also common. Many crystals, particularly those doped with rare earths, have a high-temperature peak near  $150^\circ\text{C}$  and a smaller peak at about  $60^\circ\text{C}$ . Complete dosage curves were not generated for the rare-earth-doped crystals, so it is not certain that the curves shown in Fig. 2 represent saturation conditions. This could account for some of the variations of peak temperature. The glow curves from other samples in each batch were very similar to the curves shown in the figures but there were some differences in relative intensity.

### TL Intensity versus uv Dose

Dosage curves were generated for a number of crystals by exciting with about  $13 \text{ mW/cm}^2$  from the full deuterium source for times ranging from 0.01 seconds to several hours. The data were taken in random order and numerous check runs were made to minimize experimental errors. The areas under the glow peaks were plotted on a log-log plot. On all of the dosage plots each unit of area corresponds to  $1 \text{ cm}^2$  of area on the data charts adjusted to the  $10^{-7}$ -A scale of the electrometer. These numbers can be related to the number of radiative transitions as will be shown in a later section.

The dosage curves for the crystal labeled OR2 are shown in Fig. 3. The growth rate for the total glow is nearly linear until saturation. Several

TABLE I. Physical characteristics of some ThO<sub>2</sub> samples.

Sample No.	Source	Physical appearance	Growth method dopant	Distinguishing optical properties
OR1 (3, 11)	ORNL batch No. 1	Less than 3 mm on edge jagged with facets clear, colorless	Li <sub>2</sub> O · 2WO <sub>3</sub> Pure	Bright TL green emission (Er)
OR2 7, 8, 9, 10	Same	Same	Same	Bright TL, line emission sharp excitation, absorpt. cutoff at 215 nm
OR4 5, 6	Same batch No. 2	Same	Same Ca doped	Weak TL narrow excitation additional peaks
FI1	Franklin Institute	1 × 0.5 × 0.3 cm polished faces light brown	Arc grown	Bright TL emission towards red
FI2	Same	1 × 0.5 × 0.3 cm polished faces colorless	Same	Bright TL blue and red emission
PE2 (PE1)	Perkin- Elmer, Inc.	0.5 × 0.5 × 0.3 cm polished faces tan color	Lead flux	Overlapping TL peaks broad emission
ESP1	Electronic Space Products	White powder	Less than 10-ppm impurities	Broad, overlapping TL peaks
N1 (N2)	Norton Company	1 × 1 × 0.2 cm polished light brown	Arc grown reactor grade starting material	Self-excitation red-shift emission
OR12, 13 14, 15	ORNL	Clear, colorless	Li <sub>2</sub> O · 2WO <sub>3</sub> -B <sub>2</sub> O <sub>3</sub> Er	Bright TL Er line emission
OR16, 17 18	Same	Red	... Pr	Weak TL
OR19, 20	Same	Very small red	... Tb	Negligible TL green fluorescence
OR21, 22 23	Same	Clear, colorless	... Eu	Bright TL red emission
OR24, 25 26	Same	Colorless, cloudy easily shattered	Li <sub>2</sub> O · 2WO <sub>3</sub> Dy	Bright TL line emission
OR27, 28 29	Same	Very small yellow	... Nd(Gd)	Weak TL
OR30, 31 32	Same	Clear, colorless	Li <sub>2</sub> O · 2WO <sub>3</sub> -B <sub>2</sub> O <sub>3</sub> Yb	Moderate TL emission: two broad bands
OR33, 34 35	Same	Clear, colorless	... Tm	Moderate TL broad emission

peaks show quadratic growth initially followed by linear growth and then saturation. The relative magnitudes of the peaks change drastically between low- and high-dose levels. Saturation is attained after nearly the same dose level for all peaks, but there are some not too subtle differences.

Dosage curves for OR2 were also generated with monochromatic excitation at 210 nm. The growth forms were very similar to those shown in Fig. 3.

The most outstanding difference was that the -14 °C peak saturated relatively much more quickly. The differences of excitation times required were consistent with the differences in excitation intensity at the sample and with the fact that the excitation spectra are sharply peaked at 210 nm for the undoped thoria crystals.

We observed that the temperatures of the principal peaks underwent orderly shifts as a function of

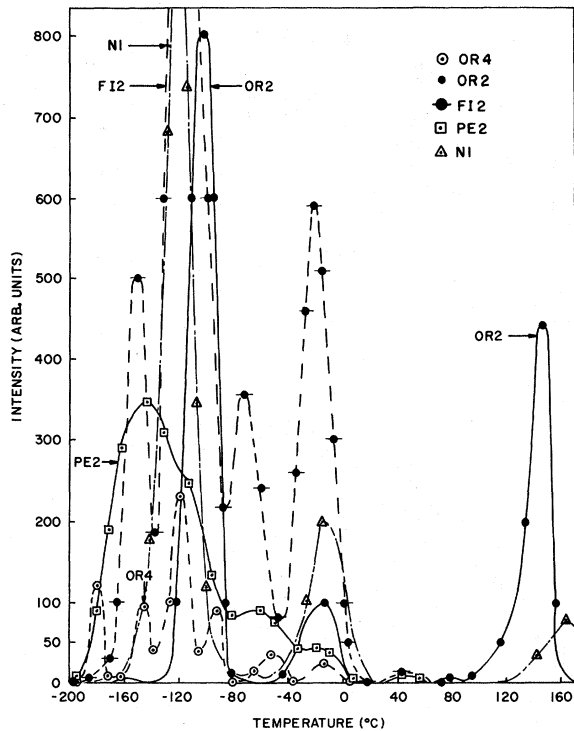


FIG. 1. Composite glow curves of some  $\text{ThO}_2$  single crystals.

dose. Fig. 4 is a semilog plot of the change of peak temperature from the peak temperature observed at saturation conditions (60 min, full source) as a function of excitation time. The  $-15$  and  $-103^\circ\text{C}$  peaks show regions of uniformly decreasing peak temperature with increasing dose that are possible indications of strong self-retrapping.<sup>14</sup> The  $149^\circ\text{C}$  peak was not observed at low-dose levels; instead, a peak at about  $115^\circ\text{C}$  was observed. All intermediate doses yielded a single peak which shifted upward with dose, although two individual peaks were resolved in some cases where the excitation was with monochromatic light. The breaks in the temperature shift for the  $149^\circ\text{C}$  peak correspond to the breaks in the dosage curve, and the region of maximum shift rate corresponds to the region of quadratic growth with dose. The regions of uniform downward shifts in peak temperature for the  $-103$  and  $-15^\circ\text{C}$  peaks seem to correspond rather well with the regions where the dosage curves grow at approximately linear rates.

The dosage curves for the crystal N1 are shown in Fig. 5, and they have growth behavior and relative peak magnitudes for moderate to high dose that prove under close examination to be generally consistent with the behavior indicated in the dosage curves for OR2 and the other Oak Ridge crystals. The major difference is that the usual second-

order growth with low dose is masked by the self-excitation which results from the natural radioactive decay of thorium. It is most apparent for this crystal because the crystal is larger than usual. The only other major differences are that the saturation level for the  $-14^\circ\text{C}$  peak is unusually high with respect to the  $166^\circ\text{C}$  peak which corresponds to the  $149^\circ\text{C}$  peak for OR2, and that the growth for the  $-14^\circ\text{C}$  peak is more nearly linear than is usual.

The self-excitation of N1 is a result of the natural decay of thorium which emits 3.98-MeV  $\alpha$  particles and 0.055-MeV  $\gamma$  rays with a half-life of  $10^{10}$  yr. The growth rate for the  $-119^\circ\text{C}$  glow peak is shown in the lower right-hand corner of Fig. 5. The self-excitation is clearly responsible for the low-dose TL because the minimum time required during a normal run to turn the sample around to face the photomultiplier, etc. is about 2 min. Finch *et al.* have also observed self-excited thermoluminescence in thoria crystals grown by them.<sup>7</sup> Linares has reported that the radioactive decay does not degrade the fluorescence of rare-earth-doped thoria.<sup>8</sup>

The dosage curves for several of the other Oak Ridge crystals are similar to the curves in Fig. 3. In general, the initial growth of the dosage curves for the peaks near  $-160$ ,  $-103$ ,  $80$ , and  $150^\circ\text{C}$  tends to be quadratic with time. The  $-103$  and  $150^\circ\text{C}$  glow peaks usually exhibit abrupt changes

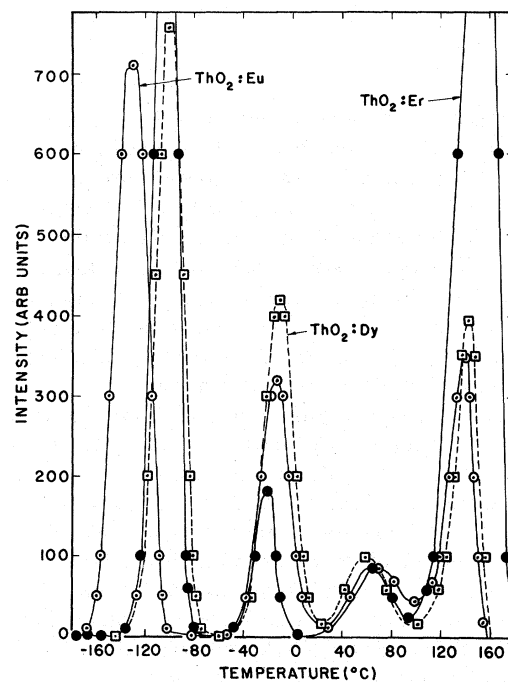


FIG. 2. Composite glow curves of  $\text{ThO}_2$  single crystals containing Eu, Dy, or Er.

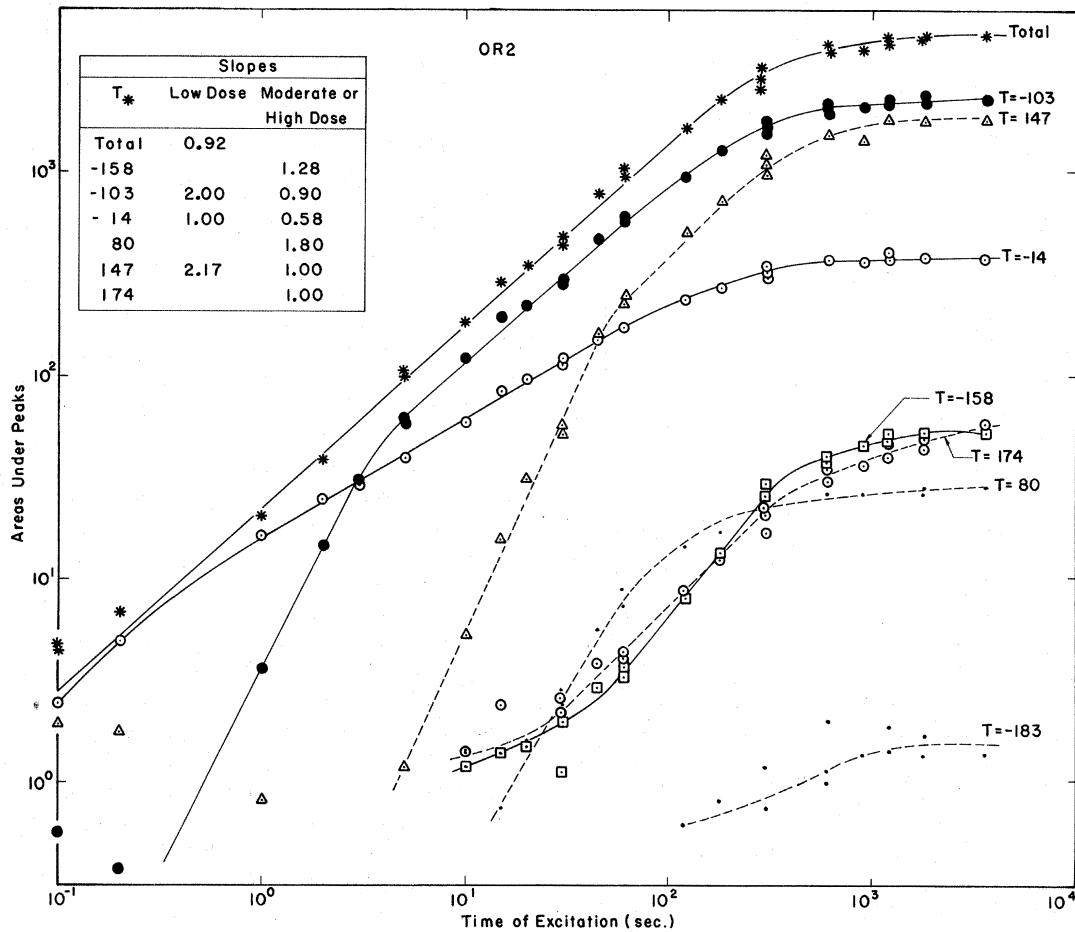


FIG. 3. Dosage curves for  $\text{ThO}_2:\text{OR2}$  (full-source excitation).

in growth behavior which occur at different irradiation times for each peak. The changes are followed by about a decade of approximately linear growth prior to saturation. The larger crystals, or those with greater general impurity content, have less tendency to show regions of quadratic growth, but this can be accounted for by the fact that in a relative sense, low-dose data were not obtained because of weak TL or because of masking by the self-excitation discussed above.

Quadratic growth regions are sometimes explained by two-step excitation processes,<sup>15</sup> but that explanation does not apply in this case. The appropriate explanation, which is based on the over-all study, is the following: Luminescence-active hole traps  $N_a^i$  and electron traps  $N_d^i$  are populated at a linear rate during the initial excitation time  $t$ . Then, for example, when the  $m^i(t)$  electrons which partially occupy the  $N_d^i$  electron traps are thermally activated, they can be retrapped by the  $N_d^{i>j} - m^{i>j}(t)$  unpopulated deep electron traps or by  $h(t)$  populated hole traps. Since the number of

unpopulated deep electron traps does not change much with time initially, the TL intensity is proportional to  $m^i(t)h(t)$ , or to  $t^2$ .

We return now to the general tendencies for glow peaks and state that the TL peaks near 174 and 220 °C and the total glow tend to have linear growth curves. The glow-peak behavior is explained if there is no appreciable retrapping by deep traps during these highest-temperature glow peaks, so that the same fraction of the thermally activated charges will recombine radiatively at all dose levels. The linear growth of the total glow is explained by the fact that all filled luminescence active hole traps will have recombined with electrons when all of the trapped electrons have been thermally activated regardless of the dose level. The luminescence hole traps form the most tightly bound states of those observed.

The dosage curves for the TL peaks near -14 and -180 °C tend to have broad regions of sub-linear growth, and in accordance with this, the -14 °C peak frequently is the dominant TL peak at

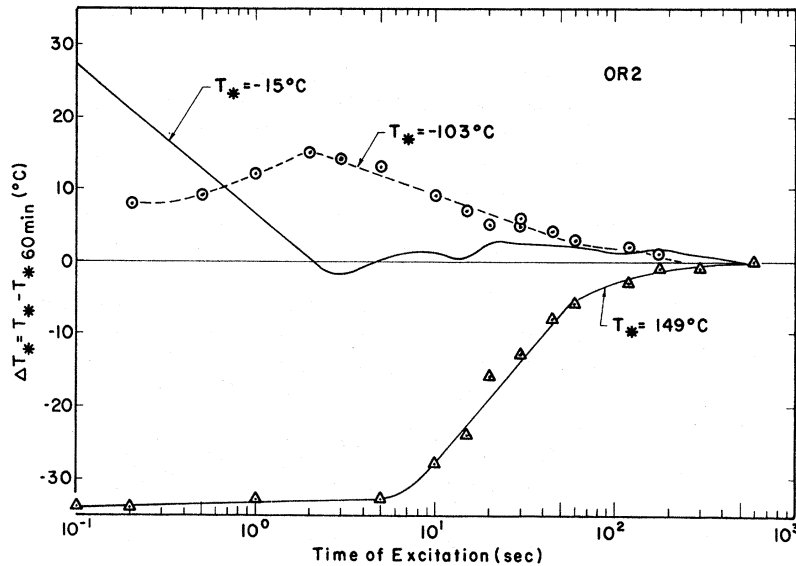


FIG. 4. Shifts in the TL peak temperatures with dose for  $\text{ThO}_2:\text{OR}_2$ .

low-dose levels. We cannot account for the sublinear growth except by postulating a series of traps which have similar energy levels and which reach maximum states of population in turn, but sublinear growth has sometimes been explained by complex processes.<sup>15</sup>

As stated at the beginning of this section, most dosage curves indicate that most of the glow peaks saturate at about the same time. In most cases, however, the  $-14$  and  $80^\circ\text{C}$  TL peaks do saturate before the others and there are cases where the difference is as much as an order of magnitude. There are cases where the  $-14$ ,  $-53$ , and  $-90^\circ\text{C}$

glow peaks reach a maximum at some dose level and then decay. There are also cases where all peaks except the one near  $149^\circ\text{C}$  have saturated.

We will conclude later that the excitation process in our measurements on thoria occurred mainly by excitation of electrons from the  $\text{O}^{2-}$  band to the  $\text{Th}^{3+}$  band. The resulting holes and electrons are subsequently trapped. Therefore, the saturation levels and growth behavior for glow peaks depend on how the limiting equilibrium levels for charge distributions depend on the electron and hole trap densities. During the irradiation, the equilibrium levels for free electrons and holes and for

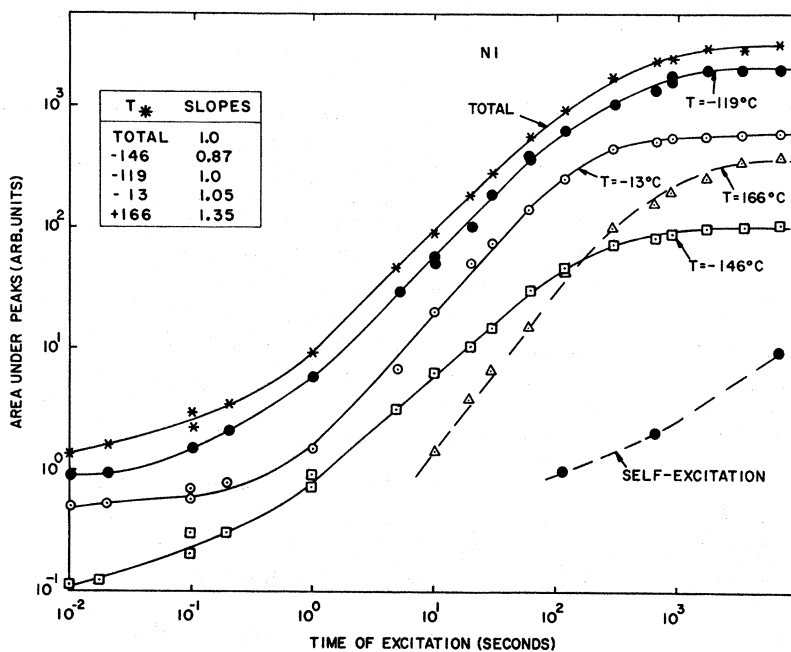


FIG. 5. Dosage curves for  $\text{ThO}_2:\text{N}_1$ .

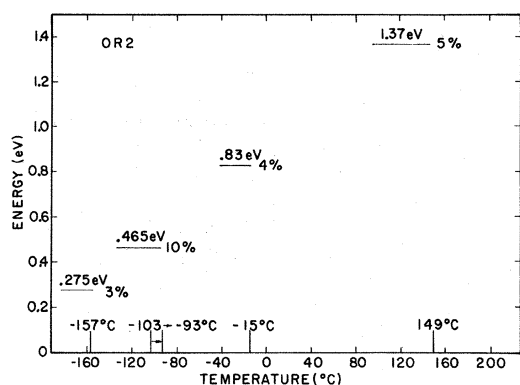


FIG. 6. Thermal activation energies of electron traps from initial-rise data for  $\text{ThO}_2:\text{OR}_2$ .

trapped electrons and holes depend on the cross sections for optical excitation of the electrons of the oxygen band and on those for the trapped electrons and holes, on the capture cross sections for empty hole and electron traps, and on the recombination cross sections for filled electron and hole traps. Some of the data presented later on will indicate relative values for some of the capture and recombination cross sections and for the optical-activation probabilities.

#### Energy and Frequency-Factor Analysis

Thermal-activation energies and frequency factors were calculated from glow-curve data by methods which utilized the initial rise, inflection, and low-temperature half-width points of glow curves. The calculations were made with a computer according to monomolecular and bimolecular models as discussed by Land.<sup>11,14</sup> The general indications are that peaks are too broad to be described by the simple models, either because of overlapping processes or because of strong self-retrapping; for this reason, it is believed that the energy and frequency factors obtained by the initial-rise analysis are the most appropriate of those obtained.

The results of the initial-rise calculations for OR2 are shown, as an example, in Fig. 6. Each rise yielded from 4 to 12 data-point pairs (temperature and intensity), and the energy and frequency factors were calculated from consecutive point pairs and from the first point pair and all others. A large number of rises were recorded and the average value of the calculated energies for the monomolecular model was plotted versus the average temperature of each rise. The plotted points formed well-defined plateaus which are represented by the horizontal lines in the figure; and the scatter in average values is indicated by the accompanying percentages. The TL peak temperatures of the traps involved are shown as

vertical marks along the abscissa; the upper temperature of  $-93$  for the  $-103$  °C peak corresponds to the peak in glow intensity obtained on the final rise that was used in the analysis of the peak. There are upward shifts in peak temperatures for most TL peaks in thoria as they are decayed by the generation of initial-rise data; but the shifts are more prominent for the large peaks since they can be decayed over more orders of magnitude. The shifts with decay are considered to be a result of peak complexity or strong self-retrapping. The latter is a good possibility in the case of the  $-103$  and  $-14$  °C peaks because of the downward shifts with increasing dose that were described in the previous section.

Table II shows the results of energy and frequency-factor calculations for six crystals by all three methods. The terms rise and fall used in the table refer to the low- and high-temperature sides of a glow peak, respectively. It can be seen that in most cases, the energies calculated by utilizing the inflection or half-width points are considerably lower than those calculated from the initial rise of a glow curve. This means the curves are too broad to be described by simple analytical models. There is fairly good agreement between methods for the  $-157$  °C peak, however; the higher than usual values obtained by the inflection points and half-width points for OR4 occurred because of the extraordinary resolution of glow peaks which can be seen in Fig. 1 for this crystal. The table indicates generally good agreement in the initial rise energies for glow peaks that are common to different crystals.

The  $149$  °C peak of OR2 and those which correspond to it are obviously truncated in some cases and they are obviously narrower than peaks which commonly occur in the neighborhood of this temperature. That is the reason that the energies from the high-temperature inflection-point calculations are so high. In attempting to account for the truncation, we considered the possibility that luminescent recombination centers were exhausted or that there might be a thermal quenching of the thermoluminescence that would correspond to a thermal quenching of fluorescence. Neither of these explanations prove to be satisfactory, and the explanation which is based on data which will be presented later is that the truncation is a result of thermal activation of holes which recombine with some of the remaining trapped electrons.

#### Emission (TL and Fluorescence)

The TL emission spectra of the crystals were measured first with the filter wheel<sup>9</sup> which is, in effect, a high-sensitivity low-resolution spectrometer. The TL emission spectra of the crystals obtained from the Franklin Institute, Perkin-Elmer,

TABLE II. Thermal activation energies and frequency factors for TL peaks from six ThO<sub>2</sub> single crystals according to initial rise, inflection points, and half-widths.

T <sub>*</sub>	Sample	Initial rise		Inflection points						Half-widths					
		Monomolecular		Monomolecular		Bimolecular		Monomolecular		Bimolecular					
		E	log <sub>10</sub> φ	Rise	Fall	Rise	Fall	Rise	EM	Rise	EB				
-157	OR2	0.275	11	0.232	9	0.260	10	0.297	12	0.415	17	...	...	...	...
-157	OR7	...	...	0.265	11	0.229	9	0.303	12	0.397	17	0.25	10	0.30	12
-156	OR8	...	...	0.263	10	0.251	10	0.301	12	0.391	16	0.28	11	0.32	13
-148	OR4	...	...	0.355	13	0.254	9	0.392	15	0.461	18	...	...	...	...
-103	OR2	0.465	13	0.264	6	0.216	5	0.325	8	0.358	9	...	...	...	...
-111	OR1	0.45	13	0.278	7	0.213	5	0.324	9	0.394	11	0.27	7	0.30	8
-101	OR7	0.48	13	0.287	7	0.217	5	0.342	9	0.360	9	0.28	7	0.33	9
-100	OR8	0.48	13	0.281	7	0.216	5	0.341	9	0.359	9	0.27	7	0.31	8
-122	N1	0.40	10	0.249	7	0.160	4	0.300	9	0.272	8	0.24	7	0.28	8
-122	OR4	...	...	0.457	14	0.405	12	0.513	16	0.729	23	...	...	...	...
-15	OR2	0.83	15	0.609	10	0.568	10	0.664	12	1.01	18	...	...	...	...
-09	OR1	0.86	15	0.624	11	0.579	10	0.738	13	0.980	18	0.68	12	0.79	14
-14	OR7	0.85	15	0.646	11	0.572	10	0.776	14	0.949	17	0.73	13	0.79	15
-13	OR8	0.85	15	0.577	11	0.565	10	0.741	13	0.939	17	0.66	11	0.76	14
-13	N1	0.75	12	0.428	7	0.296	4	0.530	9	0.506	8	0.46	8	0.53	9
-17	OR4	...	...	0.797	14	0.607	10	0.960	18	1.03	19	...	...	...	...
+146	OR2	1.37	15	1.63	18	2.93	34	2.07	23	4.87	57	...	...	...	...
162	OR1	1.39	15	1.31	14	1.43	15	1.60	17	2.38	26	1.44	15	1.67	18
150	OR7	1.37	15	1.62	18	1.54	17	1.90	21	...	...	1.62	18	1.89	21
153	OR8	1.32	15	1.38	15	1.95	22	1.74	19	3.22	36	1.53	17	1.78	20
166	N1	1.25	13	1.13	11	0.970	9	1.38	14	1.72	18	1.22	13	1.42	15

and the Norton Company extended over most of the visible spectrum. We observed several glow peaks that were split into several components, each with different emission spectra. In some cases, the submerged peaks were consistent with the observation of multiple peaks at low-dose conditions. We also observed that the emission spectra were different for different glow peaks; i. e., for the crystal N1, the -119 °C peak had an emission maximum at 440 nm and the 166 °C peak had an emission maximum at 580 nm. We also observed some shifts of spectra between the low- and high-temperature sides of a glow peak.

The emission spectra of the Oak Ridge crystals were the characteristic line spectra of trivalent rare-earth ions. These spectra were measured either by placing the monochromator between the sample and the photomultiplier and scanning manually or by scanning narrow selected regions of the spectrum with a Spex 1700 spectrometer. The fluorescence of some of the Oak Ridge crystals was also measured with the spectrometer.

The fluorescence of OR2 at 20 °C is shown in Fig. 7 where the excitation was with 210 nm and it is characteristic of trivalent erbium. (Spectral lines may be shifted by 2 or 3 Å as the spectrometer was not calibrated.) High-resolution measurements with the spectrometer showed that the lines in the TL spectrum corresponded to those for the fluo-

rescence shown in Fig. 7. Low-resolution measurements with the filter wheel showed that the shorter wavelengths near 525 nm were enhanced for the high-temperature glow peaks. The enhancement was greater for OR1 than for OR2.

The TL emission spectra from some of the other rare-earth-doped crystals are shown in Fig. 8. Most of the spectra were analyzed with low resolution only, but one can see that each rare-earth dopant produces a unique TL emission spectrum

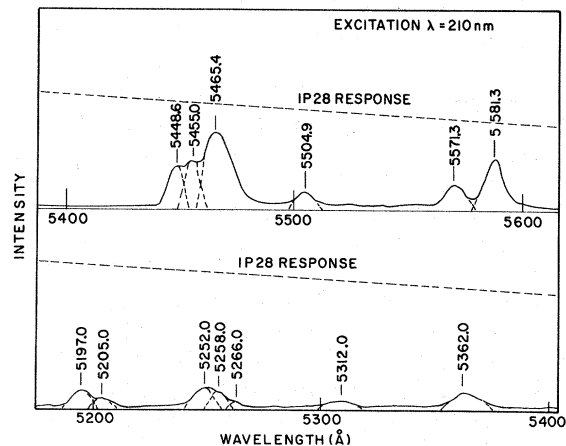


FIG. 7. Fluorescence emission spectra for ThO<sub>2</sub>:OR2 at 20 °C with 210-nm excitation.

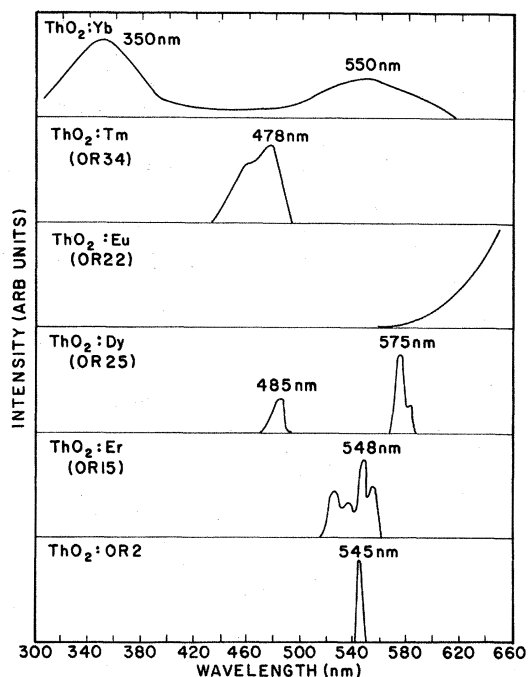


FIG. 8. TL emission spectra for some rare-earth-doped  $\text{ThO}_2$  crystals.

and the TL spectra agree with the fluorescence spectra as reported by Linares or in the text of an article by Trofimov.<sup>16,17</sup> One exception was a crystal which was doped with 20-ppm wt Yb; it has emission which is characteristic of  $\text{Ce}^{3+}$  which is also present at 5 ppm wt. If one refers back to the glow curves in Figs. 1 and 2 it can be seen that those for the rare-earth-doped crystals are very similar; this suggests that the electron trapping states are independent of the rare earths.

The fluorescence spectra from the rare-earth-doped crystals are in many cases very bright. Some of the spectra are rather complex in that they have strong temperature dependences and multiple excitation spectra. These observations are incomplete and will be published separately.

The  $\text{Er}^{3+}$  ions in OR2 occupy primarily  $\langle 111 \rangle$  axial and cubic sites.<sup>5</sup> It would be logical for the axial species to be associated with oxygen vacancies and to provide electron traps, but most of the data argue against these as dominant electron traps. The cubic sites do provide hole traps either on the rare-earth or on neighboring oxygen ions.<sup>5</sup> When the electrons recombine with the holes the characteristic trivalent luminescence is emitted. We note that this requires exception from the rule which states that dipole transitions are forbidden for trivalent rare-earth ions which occupy sites having inversion symmetry.<sup>18</sup> This is consistent with the observations of Linares for thoria

fluorescence and with those of Merz on the thermoluminescence of rare-earth-doped  $\text{CaF}_2$ .<sup>16,19</sup>

The work which we insert at this point was done after Rodine's thesis was completed; it was done as part of the effort to determine whether thermal quenching of rare-earth fluorescence in the neighborhood of 150 °C could explain the truncation of TL peaks near 150 °C; to determine if there was evidence of valence changes for rare-earth ions; and to determine if the higher temperature TL peaks could be excited directly by x-rays. The first two indications are negative, and the last is positive.

We mounted a group of the crystals from the batch which yielded OR1, OR2, OR7, and OR8 and studied the x-ray (35-keV cobalt, transmitted through aluminum foil) induced fluorescence as a function of temperature and trap population. We observed that the fluorescence at 77 °K was due almost entirely to the  $\text{Gd}^{3+}$  line group near 300 nm, whereas at higher temperatures the emission was due to the line groups which are associated with  $\text{Er}^{3+}$ . The temperature dependence of the total emission and of the major line groups are shown in Fig. 9; the component intensities are corrected for the spectral response of the 1P28 photomultiplier, which is about 2–1 for the 300- and 535-nm regions, respectively. The figure shows that the  $\text{Er}^{3+}$  emission increases with temperature and that the line group near 525 nm increases most rapidly and becomes dominant; the intermediate growth rate for the 535-nm line group is not shown explicitly because the growth was masked under the low-resolution conditions employed in the experimental setup. These observations are consistent with the relative increases in the emission of shorter wavelengths with increasing temperature that was noted for the higher-

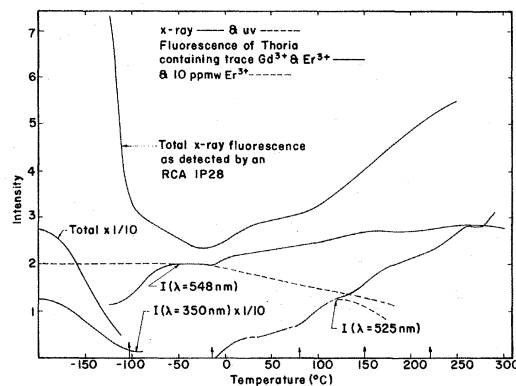


FIG. 9. Temperature dependence of the fluorescence from  $\text{ThO}_2$  with trace Gd and Er and with 10-ppm wt Er under x-ray or uv excitation. The vertical arrows indicated the temperatures of major TL peaks.

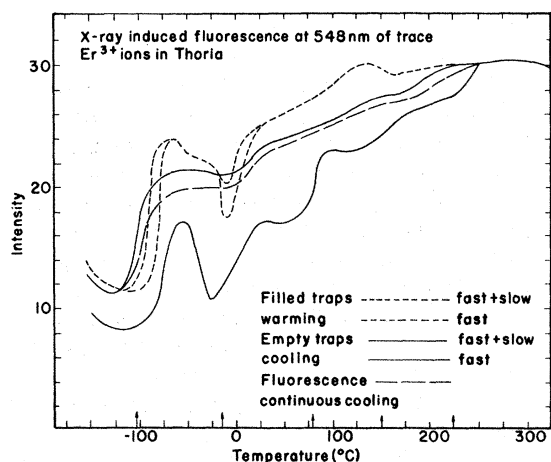


FIG. 10. Short-time behavior of the x-ray-induced fluorescence of  $\text{ThO}_2$  with trace  $\text{Er}^{3+}$ . The vertical arrows indicate the temperatures of major TL peaks.

temperature glow peaks of OR1 and OR2. The thermal quenching of the  $\text{Gd}^{3+}$  fluorescence corresponds to the fact that  $\text{Gd}^{3+}$  EPR lines of OR1 can be decayed by uv excitation below but not above the temperature where quenching occurs.<sup>4</sup>

We also include in Fig. 9 the temperature dependence of the fluorescence of a thoria crystal containing about 10 ppm wt of erbium, where the excitation was with 260-nm uv. The emission intensity is constant below 0 °C for the 545 line group. Apparently, the major decrease near -100 °C of the x-ray induced 545-nm  $\text{Er}^{3+}$  emission from the undoped thoria crystals results because of competition from the  $\text{Gd}^{3+}$  ions. (There was no evidence of  $\text{Gd}^{3+}$  in OR2.<sup>4,5</sup>) The low-temperature behavior is therefore basically the same for the trace and 10-ppm  $\text{Er}^{3+}$  in thoria. At higher temperatures, however, it can be seen that the uv fluorescence of crystals with 10-ppm wt of  $\text{Er}^{3+}$  begins to decrease at much lower temperatures than does the x-ray induced fluorescence of trace  $\text{Er}^{3+}$ . We expect that the difference is due to concentration rather than means of excitation.

There was no significant intensity difference observed for the  $\text{Gd}^{3+}$  300-nm x-ray-induced fluorescence at 77 °K for zero and saturation TL excitation dosages. At higher temperatures where  $\text{Er}^{3+}$  emission was dominant, the rather complicated behavior illustrated in Fig. 10 was observed. The broken curve describes the continuous emission at 548 nm, which was observed while cooling at approximately 0.5 °C/sec. The dotted curves show the fluorescence behavior that was observed while heating from a filled trap condition; the x-ray excitation was switched on and off periodically in order to separate the fluorescence from the TL. The x-ray excitation was also switched

on and off at various temperature plateaus in heating and cooling schedules. We observed that the fluorescence intensity had periods of rapid growth (less than one second) and slow growth (usually less than one minute) which were dependent on the trap populations and on whether the fluorescence was observed on the high- or low-temperature side of a glow peak. The dotted curves show that there is a characteristic behavior on the high-temperature side of saturated glow peaks such that there are marked increases in the fluorescence intensity and a large slow component in the transition region; whereas, there are characteristic decreases in the fluorescence on the low-temperature side, and no slow component. The solid curves show the behavior of the fluorescence on temperature plateaus while cooling from an annealed condition; in this case, the initial fluorescence measured anywhere within the region where glow peaks occur always has a slow rise component. If the measurement is made repeatedly at a temperature between glow peaks the fast-rise component grows toward a limiting value while the observed portion of the tail of the slow-rise component decreases toward zero. This change is complete after a low total dose of x rays. When the measurements are made near a glow peak we observe phosphorescence with a symmetric rise and fall and with fast and slow components having comparable magnitudes.

Our interpretation of the above observations, without attempting any detailed explanation of processes, is that the x-ray fluorescence is excited by the formation of electron hole pairs. We suppose that the holes are captured by, or selectively created at, oxygen ions in the neighborhood of rare-earth ions, and that the latter are excited to luminescence when free electrons recombine with the holes. This description can account for the quenching of the  $\text{Gd}^{3+}$  fluorescence by the thermal activation of gadolinium-associated nonparamagnetic holes; paramagnetic holes are observed to anneal in the appropriate temperature range in OR2 but they are not associated with Gd since none was present.

The EPR measurements indicate that a substantial reduction in the amount of  $\text{Gd}^{3+}$  and  $\text{Er}^{3+}$  can be achieved with uv excitation at 77 °K.<sup>4,5</sup> There is no obvious change in the x-ray-induced fluorescence emission with respect to total and relative intensities of individual line groups that correlates with substantial filling of traps; the slow-rise components of Fig. 10 correspond to very low doses of TL excitation. We conclude, therefore, that there is relatively little direct excitation of  $\text{Gd}^{3+}$  and  $\text{Er}^{3+}$  ions. This in turn means that any direct x-ray excitation of divalent or quadrivalent rare-earth ions would be weak so that their observation

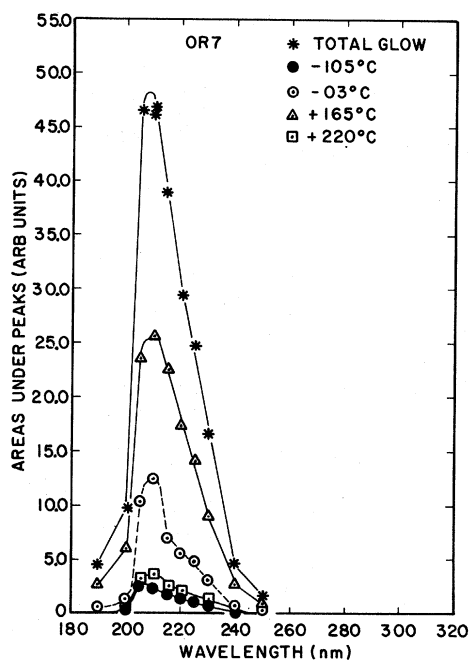


FIG. 11. Excitation spectra for TL of  $\text{ThO}_2$ :OR7.

would require more care.

We considered the possibility of determining the presence of divalent or quadrivalent rare-earth ions through fluorescence by looking for new spectra and changes in the intensity of the trivalent spectra with changes in trap occupation while exciting with uv that is less energetic than the band gap, since this excitation condition should increase the relative importance of direct excitation of the rare earths; unfortunately, the fluorescence intensity for the undoped crystals is too weak under these conditions for good measurements so that we could not determine whether the holes are on the rare earths or neighboring oxygen ions.

#### Excitation Spectra and Optical Absorption

The excitation spectra were measured by irradiating the crystals with the same number of photons at each wavelength. The dosage levels were very low compared to saturation doses and were different for each wavelength. The dosage curves showed that at low-dose levels the relative strengths of the peaks change rapidly as a function of dose; the effects of dose are therefore included in the excitation spectra, but do not prevent the basic interpretation of the results.

We determined the excitation spectra of four of the undoped Oak Ridge crystals and of one europium-doped crystal. The spectra for all of the undoped crystals were narrow with maxima at about 210 nm and were skewed toward the long wavelengths. The amount of skewness and the relative

strengths of the individual peaks varied among crystals. The excitation spectra for  $\text{ThO}_2$ :Eu were similar to the undoped crystals except that the peak was at 220 nm; we would expect similar results for the other rare earths.

The excitation spectra for OR7 are shown in Fig. 11, and it can be seen that there are some differences in the spectra for individual peaks. The units for the areas under the peaks are the same as for the dosage curves. The total glow at the maximum is approximately equal to that obtained after 50 sec of full-source excitation. The strength of the 165 °C peak is anomalously large in this case, but usually the order of peaks with regard to strength is the same as in the dosage curves.

The optical transmission of OR2 was measured with a Cary 14 spectrophotometer. Very little structure or change of absorption was observed until the onset of the uv cutoff below 240 nm. At 215 nm, the absorption became too strong to follow. A uv cutoff at 215 nm corresponds to a band gap of 5.75 eV, which is larger than that previously reported.<sup>8,13,20</sup> Thus, it is clear that the excitation spectra indicate that the most efficient process is direct transition across the band gap.

#### Bleaching

We conducted bleaching studies on several crystals at 77 °K in an attempt to determine the optical activation energies for the traps. For each run, the crystal was first excited to saturation with the full deuterium source; then it was exposed to a second "bleaching" dose from the full tungsten source or with the monochromator with the visible or infrared grating. The areas under the glow curves at saturation conditions with no bleaching were taken as the norms in this experiment.

In Fig. 12, the percentage of glow remaining after bleaching OR1 with the full tungsten source is plotted as a function of the bleaching time. It can be seen that the lower the peak temperature, the more rapidly it bleaches. The short-time decay for all peaks follows an exponential form, i. e.,  $dI/dt \propto I$ . Figure 13 shows the results of bleaching OR1 with the same number of photons for different wavelengths in the visible and infrared. These results indicate that the lower the peak temperature the more rapidly it bleaches. Some of the higher-temperature TL peaks show enhancement because at the lower bleaching dose levels, re-trapping of charge liberated from shallower traps (regenerative re-trapping) more than compensates for the loss of charge by optical bleaching. Longer exposures show that all of the traps associated with TL peaks below 0 °C are bleached by 1- $\mu$  light.

The re-trapping of optically and thermally activated charges complicates the meaning of the bleaching-vs-wavelength curves; however, the

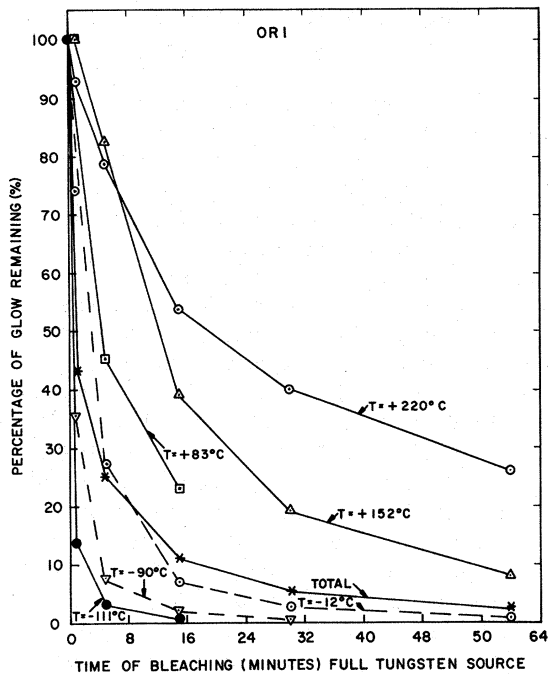


FIG. 12. Bleaching of TL with a tungsten source for  $\text{ThO}_2:\text{OR1}$ . 100% corresponds to the response with a saturation dose and no bleaching.

general effect of regenerative retrapping is to increase the maximum slope of the curves in Fig. 13 so the increase in bleaching efficiency with decreasing wavelength is as great if not greater than indicated. Retrapping effects could be eliminated by exciting and bleaching at a temperature just below each TL peak, but this would be quite time consuming, and the data in Fig. 13 are sufficient to show that optical activation energies are

not very well defined.

Figure 14 is an excitation (bleaching) curve, at  $20^\circ\text{C}$ , for a crystal of  $\text{ThO}_2:\text{Er}$  which appeared in a report by Finch *et al.* for the TL peaks above  $20^\circ\text{C}$ .<sup>7</sup> The crystal was given a 10-sec "predose" of 240-nm light and then another dose for 10 sec with another wavelength which yielded the curve for the change in the TL intensity resulting from the second dose. The specific shape and crossover point for this curve depend on the intensity distribution for the light source and monochrometer used, and on the trap populations achieved for the peaks occurring between 20 and  $150^\circ\text{C}$  at very low dose; at higher doses the crossover point must shift below 215 nm according to our observations because it was only with x-rays (30-keV cobalt target passed through aluminum foil) that we got appreciable amounts of trapped charge by direct excitation at  $20^\circ\text{C}$ .

One can see that our  $77^\circ\text{K}$  excitation and bleaching curves belong to a set containing curves similar to the one in Fig. 14. Our excitation is a special case with zero pre-excitation so there is no bleaching and no crossover; our bleaching conditions were for crystals which had been saturated with the full deuterium source and, had the data been extended into the uv, we would have found crossover points for some traps, but perhaps not for all.

We have done a small amount of excitation and bleaching of thoria at room temperature, and this was stimulated by the EPR data of Neaves and Tint which are discussed in the EPR section. They observed that the electron traps responsible for the glow peaks near  $149^\circ\text{C}$  are occupied by retraining from the  $-103$  and  $-14^\circ\text{C}$  TL peaks; if the traps were populated in this manner and the crystal was then cooled to  $87^\circ\text{K}$  and irradiated as usual with the

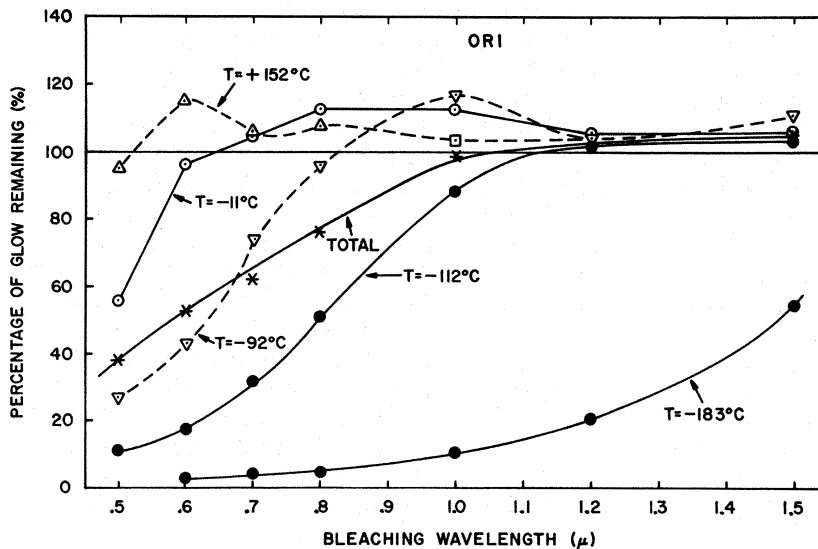


FIG. 13. Bleaching of TL vs wavelength for  $\text{ThO}_2:\text{OR1}$ . 100% corresponds to the response with a saturation dose and no bleaching.

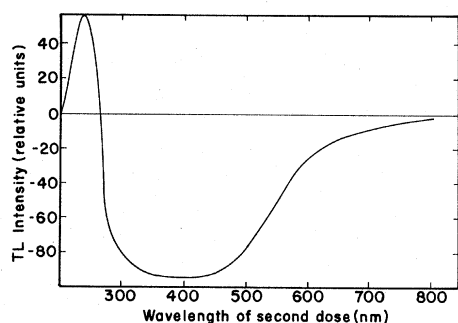


FIG. 14. Change in TL intensity for  $\text{ThO}_2$  for excitation with a 10-sec dose after a 10-sec predose at 240 nm as observed by Finch *et al.*

full deuterium source the EPR lines associated with these traps decayed. Subsequently, we showed that excitation with the full deuterium source at 20 °C produced no appreciable TL and in fact that re-trapped charge was removed from the 149 °C traps. Bleaching occurred for all uv wavelengths greater than 215 nm, and in all cases the uv bleaching was more effective for the 149 °C peak than for neighboring shoulders.

Semilog plots of the bleaching data of Neaves and Tint show that the decay of the two 149 °C electron resonances under uv at 87 °K go as  $\ln S = -\alpha t$ , with  $\alpha(A) = 0.0135 \text{ sec}^{-1}$  and  $\alpha(B) = 0.004 \text{ sec}^{-1}$  for retrap A and B, respectively. Simple exponential decay is considered most likely at low temperatures since trapping by shallower traps decreases the probability of self-retrapping by the 149 °C traps.

We observed that the 149 °C TL for a 30-min dose with the full deuterium source at 77 °K is reduced by a factor of 15 by a 30-min dose at 20 °C, while that for a 1-min dose at 77 °K is reduced by a factor of 90 for the same bleaching condition. The decay of the 149 °C TL is not expected to be a pure exponential because of the difference in  $\alpha(A)$  and  $\alpha(B)$ , but if the exponential decay did apply the values for  $\alpha$  would be  $0.0015 \text{ sec}^{-1}$  and  $0.0038 \text{ sec}^{-1}$ , respectively, for 30- and 1-min doses. Our values for  $\alpha$  are smaller than those of Neaves and Tint because of a smaller uv intensity, but the dose dependence is not accounted for. At 20 °C the effect of uv bleaching is presumed to be excitation of trapped electrons with subsequent recombination with trapped holes. The dose dependence we observed might be associated with the change in retrapping rate that would be associated with the fact that the occupation of the 150 °C hole traps observed by Neaves and Tint reaches a maximum after an intermediate dose, while the occupation of the luminescent recombination centers continues to increase. It should be interesting to observe the changes in

EPR absorptions at 77 °K for uv bleaching at 20 °C.

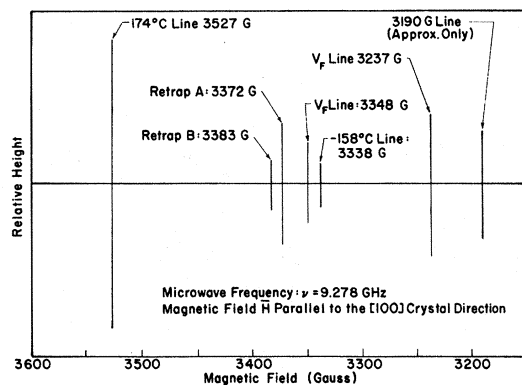
#### EPR

EPR studies were made on some of the  $\text{ThO}_2$  crystals by Neaves and Tint at the Franklin Institute Research Laboratories. The detailed results of the EPR study have been published in a technical report<sup>3</sup> and in a doctoral dissertation.<sup>4</sup> (Circumstances have prevented Neaves and Tint from preparing their work for simultaneous publication with our work.) Most of their data pertain to the crystals OR1 and OR2, and the experimental conditions of irradiation and heating were made similar to those used in the TL studies in order to simplify the correlation of data.

Prior to irradiation, the only resonance lines observed at 77 °K for OR1 were those attributable to  $\text{Gd}^{3+}$  in cubic sites. It was observed that exposing the crystal to about  $5 \times 10^{16}$  210-nm photons at temperatures between -200 and -170 °C caused the absorption line associated with  $\text{Gd}^{3+} - \frac{1}{2}$  to  $\frac{1}{2}$  transitions to decay by about 30%. The same amount of excitation at -150 °C caused less than 5% decay and none was observed at -140 °C. In a verbal communication, Tint indicated that the  $\text{Gd}^{3+}$  absorption lines were restored in two steps by heating through the -100 and 100 °C temperature ranges.

Prior to irradiation, no resonances were observed for OR2 at 87 °K. After irradiating at 87 °K, four new resonance lines were observed. When the crystals were heated to 300 °K and then cooled to 87 °K, two of the radiation-induced resonances had been annealed and two new ones were present. The six new resonances are shown in Fig. 15(a) with  $\vec{H}$  parallel to [100]. This drawing is from the report by Neaves and Tint and the labeling for most of the resonance lines reflects their association with TL peaks. Figure 15(b) is a summary of data pertaining to the states which yield the resonances. The trapped charges are identified as electrons or holes in accordance with the usual indication of a positive or negative shift  $\Delta g$  from the free-electron value of 2.0023.<sup>21-24</sup> There can be exceptions to the  $g$ -shift rule,<sup>25</sup> but its application here provides for a consistent analysis of the charge-transfer processes observed. The table indicates that no fine structure was observed for the four irradiation-induced electron resonances. In addition, these absorption lines were very narrow for temperatures near 77 °K,  $< 0.3 \text{ G}$ , and their width increased rapidly with increasing temperature. The linewidths for hole states were considerably broader near 77 °K. All of the resonances induced in OR2 were also induced in OR1.

A major part of the EPR study consisted of (a) making standard angular-variation measurements



(A) Approximate Relative Heights of the EPR Lines Seen After Irradiation of Thoria Crystal OR2

Line	Symmetry	$g_{xx}$	$g_{yy}$	$g_{zz}$	T	$T_*$	Charge
-158	axial<111>	1.9854	1.9854	1.9825	-160°C	-158°C	$e^-$
Retrap A	axial<111>	1.9619	1.9619	1.9742	148°C-103; 23,149°C		$e^-$
Retrap B	axial<111>	1.9547	1.9547	1.9682	148°C-103; 23,149°C		$e^-$
3527 G	axial<111>	1.8887	1.8887	1.8633	159°C	174°C	$e^-$
$V_F$		2.054	2.043	1.980	-127°C	-	$e^+$
3190 G		>2	>2	>2	151°C	-	$e^+$

(B) Summary of Pertinent EPR Data

FIG. 15. Some EPR data for OR2. (A) The  $\vec{H}$  [100] uv-induced spectra for OR2 after Neaves and Tint. (B) Summary of data where  $T$  is the annealing temperature for EPR lines and  $T_*$  is the associated TL peak temperature.

to determine the principal values of the  $g$  tensor and the probable sign of the charge; (b) measuring the growth of resonances with irradiation dose; (c) measuring the decay (or growth) of resonances at 87 °K with stepwise annealing which yielded curves whose derivatives are similar to TL glow curves; these EPR analogies to TL glow curves were usually narrower than the TL curves, and they usually peaked at somewhat lower temperatures, but these tendencies are partially explained by a slower heating rate and by some basic differences in the methods.<sup>4,5</sup>

Figure 15 shows that the annealing temperature for the 3338-G resonance coincides very closely with the glow peak temperature of -158 °C. The dosage curves were somewhat different in that the slope of 1.3 for the glow indicates a somewhat superlinear growth. The difference, as Tint explains in some detail on p. 111 of his thesis, probably occurs because the TL efficiency is reduced at low-dose levels because of large retrapping rates for the deeper traps. The fact that the average  $g$  values is less than 2.0023 is taken to indicate that the resonance is due to an electron. The measurements by Neaves and Tint indicate that the  $g$  tensor is isotropic, but some later measurements on OR2 by Wagner *et al.* indicate that  $g_{11} = 1.9825$  and  $g_1 = 1.9854$  with a principal axis along  $\langle 111 \rangle$ .<sup>5</sup>

The resonance lines labeled retrap A and retrap B did not appear after 87 °K uv irradiation. As the sample was heated through the -103 °C glow peak, the growth of the EPR signals was observed, and continuing heating through the leading edge of the -14 °C glow peak resulted in further growth. The strength of the retrap lines derived from the -14 °C glow with respect to the -103 °C peak equaled the ratio of the areas under the respective glow peaks. The annealing curve for the retrap lines coincided very well with the 149 °C glow peak. Neaves and Tint observed that irradiating with uv at 87 °K caused the retrap lines to decay after they had been induced by irradiating and heating to 20 °C. We observed subsequently that the 149 °C glow peak is not excited appreciably by irradiating at 20 °C with uv; and that when the retrap states are filled in the usual manner they are bleached by uv at 20 °C. Apparently the large probability for uv bleaching of 149 °C traps keeps them from being filled and this along with the fact that they are due to relatively dense trapping defects may account for their dominance in retrapping the charge which is released near -14 and -103 °C.

The 3527-G EPR line is considered to be associated with the 174 °C TL peak although the annealing temperature for the EPR line was at 159 °C. There is a shoulder on the high-temperature side of the annealing curve, and there is evidence which we will discuss later that the annealing of the 151 °C hole trap lowers the apparent annealing temperature for the 174 °C electron trap. The dosage curves for the EPR and TL were in close agreement for this trap. One particularly interesting fact is that the spin densities for the 174 °C line at saturation is about equal to the sum of spin densities for the two 149 °C retrap lines; whereas the area under the 174 °C glow peak is 25 times smaller than the area under the 149 °C glow peak. One can therefore state that the TL efficiencies for the glow peaks are different by a factor of 25.

Before we had made a careful study of the fluorescence efficiency as a function of temperature, we suspected that a rapid decrease of the  $Er^{3+}$  fluorescence in thoria in the vicinity of 150 °C could account for the decrease in TL efficiency. In turn, this could have accounted for the abnormally rapid decrease in the intensity of the high-temperature side of the 149 °C glow peak and for the factor of 25 above. The suspicion was not correct, however. Our preliminary studies of x-ray-induced fluorescence from several simultaneously mounted crystals from the batch which yielded OR1, OR2, OR7, and OR8 indicate that the total visible fluorescence is due to  $Er^{3+}$  in the range -130-300 °C and that the emission increases with increasing temperature in a rather uniform manner in this temperature range.

There are alternative explanations of the decrease in TL efficiency which is commonly indicated by the rapid cutoff of the glow peaks near 150 °C. One possibility is that the empty recombination centers are filled more rapidly than some competing nonluminescent centers so that they are almost depleted at about 150 °C. A more likely possibility which we will consider further below is that holes are thermally activated to mobile states when the 151 °C hole resonance anneals and that the mobile holes recombine with the majority of the electrons which remain in the 149 and 170 °C traps.

The  $V_F$  resonance lines anneal at approximately -127 °C and they do not correspond to a glow peak for OR2. Some other crystals do have major glow peaks which occur nearer -127 °C, but this is considered coincidental. The  $g$  tensor has approximate axial symmetry along  $\langle 100 \rangle$ , and the  $g$  values are appropriate for trapped holes. The dosage curve for this absorption is similar to that for the -103 °C glow peak in the high-dose region, but this simply reflects the approximately linear behavior exhibited in both cases. In accordance with other conclusions, we assume that the -127 °C absorption decays when holes are thermally activated to mobile states. Since this process has no noticeable effect on the intensity of the 3190-G 151 °C hole trap and the 3527-G 174 °C electron trap, we expect that the holes recombine with the electrons in the -103 and -14 °C traps.

The 3190-G 151 °C resonance line also appears to be due to trapped holes since its  $g$  value is greater than 2.04. Tint indicates that the absorption is a single line when  $\vec{H}$  is parallel to  $\langle 100 \rangle$ , and that when the field is rotated from  $\langle 100 \rangle$  toward  $\langle 110 \rangle$  the single line seems to broaden and move toward lower magnetic fields until it disappears. The annealing peak is at about 151 °C, but there is a low-temperature shoulder on the annealing curve. There is no reported evidence that the absorption by this line changes as the lower-temperature electron and hole traps are thermally activated. The dosage curve for the absorption line peaked after approximately 500 sec of approximately linear growth and then it decreased to about  $\frac{1}{10}$  of its maximum value. Tint explains in his thesis that the final equilibrium value is lower than the maximum because of the increase in the free-electron density during the excitation, which occurs as the electron traps are filled. This explanation also implies that the free-hole density decreases, and that the deep-hole traps are not filled.

The thermal activation of the 151 °C hole trap occurs after a majority of the hole-trapping luminescent recombination centers have recombined with thermally activated mobile electrons. If the majority of the thermally activated mobile holes

recombine nonradiatively with a majority of the remaining number of trapped electrons, this accounts for the unusually rapid decay of high-temperature side of the 149 °C glow peak and for the differences in the TL and EPR responses which were discussed earlier with respect to the 174 °C TL peak.

The combined TL and EPR results provide some information about the relative cross sections for electron- and hole-trapping and recombination processes. First, the only changes in EPR absorptions for deeper traps that were reported to accompany the annealing of shallower traps were those for the 149 °C retrapping lines. Secondly, the relative TL efficiency for different traps permits rough estimates for the ratio of retrapping and recombination rates. These observations indicate that the -158 °C electrons are primarily retrapped by the -103 and -14 °C traps; and this implies that the electron-capture cross sections for these traps are especially large at -158 °C because they were substantially occupied during the experiment so that capture by 149 °C electron traps or recombination with the deep erbium-associated holes would have been favored on a strictly numerical basis. The above observations also indicate that the -127 °C holes either recombine with the -103 and -14 °C electrons or that they are retrapped by the erbium-associated traps. Finally, the 150 °C holes recombine mainly with the 149 and 170 °C electrons rather than being retrapped by the erbium-associated hole traps; otherwise, the hole activation would not reduce the TL efficiency and cause the truncation of the glow peaks near 149 °C. This suggests that at 150 °C the hole recombination cross sections for the trapped electrons are larger than the trapping cross sections for the deep hole traps, since for the usual conditions there should be at least as many empty hole traps as trapped electrons.

Some further EPR studies of thoria and OR2 in particular are being conducted by Wagner, Feldman, and Murphy of Westinghouse Research Laboratories.<sup>5</sup> They have observed the  $\text{Er}^{3+}$  resonances at 4 °K, and they estimate that prior to irradiation, there are concentrations of  $\text{Er}^{3+}/\text{Th}^{4+}$  of  $1.6 \times 10^{-8}$  on  $\langle 111 \rangle$  axial sites,  $2.7 \times 10^{-7}$  on cubic sites, and a smaller concentration of  $\langle 100 \rangle$  axial sites. They reported that the  $g$  factor for the  $\langle 111 \rangle$  axial sites was nearly the same as that reported by Abraham *et al.* for  $\text{Er}^{3+}$  on  $\langle 100 \rangle$  axial sites in thoria.

They report that the EPR absorption for  $\text{Er}^{3+}$  ions in cubic sites decays with monochromatic 210-nm excitation and that there is no change observed in the noncubic sites. For other excitation conditions they do observe that the noncubic resonances decay by 20%.

TABLE III. Estimates of spin density for uv-induced lines after a near-saturation dose.

Line	Spin density for full source excitation (cm <sup>3</sup> )	Spin density for 210-nm excitation (cm <sup>3</sup> )
-158 °C	$2.5 \times 10^{14}$	$2.5 \times 10^{15}$
Retrap A	$1.5 \times 10^{14}$	$1.5 \times 10^{14}$
Retrap B	$0.6 \times 10^{14}$	$0.6 \times 10^{14}$
174 °C	$2.5 \times 10^{14}$	$2.5 \times 10^{14}$
$V_F$	$5.0 \times 10^{14}$	$5.0 \times 10^{14}$

They have observed all of the uv-induced absorptions previously described. In Table III are the estimates which they made of the spin density for uv-induced lines after a near-saturation dose.

They observed that the -158 °C  $g$  tensor was actually slightly anisotropic and that the absorption was substantially greater for 215-nm excitation with a  $\langle 111 \rangle$  axis. They also observed by x-ray analysis that OR2 was composed of at least two slightly misoriented crystals. They do not suggest that this accounts for the slightly different  $g$  factors for A and B. However, they do suggest that it may account for the fact that they resolved the 174 °C resonance into one doublet for each  $[111]$  axis.

One of the most important of their observations for the current discussion is the fact that the cubic  $\text{Er}^{3+}$  EPR absorptions decay by about one-half as a result of uv irradiation. It is possible that  $\text{Er}^{4+}$  results from hole trapping as we expect no resonance absorption for this state, and none was observed. Our observations show no evidence of fluorescence that might be associated with transitions within the  $f$  levels for this state, but they were inconclusive. It is possible that one or more oxygen ions in the neighborhood of the  $\text{Er}^{3+}$  ion can capture a hole which permits destruction of the spin resonance absorption of the  $\text{Er}^{3+}$  through an exchange interaction.

The following EPR studies on thoria are also relevant to the interpretation of this work: The earliest of the studies are those of Low and Shaltiel,<sup>26</sup> and of Abraham *et al.*<sup>27,28</sup> who measured the spectra of  $\text{Gd}^{3+}$  in cubic sites and of  $\text{Yb}^{3+}$  and  $\text{Er}^{3+}$  in cubic and axial sites. The next and most relevant EPR study until recently was by Neeley, Gruber, and Gray who observed a spectrum with  $\langle 111 \rangle$  axial symmetry with  $g_{\parallel} = 1.9739$  and  $g_{\perp} = 1.9644$  in crystals that were grown with  $\text{PbO-PbF}_2$  or  $\text{BiO}_3\text{-PbF}_2$  flux systems, after they were irradiated with either x-rays,  $\gamma$  rays, or 2-MeV electrons.<sup>29</sup> The strength of the spectrum was observed to increase when crystals were doped with erbium or lanthanum. Since no hyperfine structure was observed, it was suggested that the trivalent rare-

earth additions were compensated by unassociated oxygen vacancies which had a slight Jahn-Teller splitting and which provided the observed EPR spectrum when in a monovalent state. Later, Neaves and Tint indicated that this was the same resonance that they had labeled as retrap A.

Abraham, Finch, Reynolds, and Zelds observed that irradiation of thoria with 2-MeV electrons with  $^{60}\text{Co}$   $\gamma$ 's at 77 or 300 °K produced  $\text{Eu}^{2+}$  ions.<sup>30</sup> The EPR spectrum, which had a complex hyperfine structure, was observable only at temperatures below 77 °K, i. e., 4 °K, and the  $g$  tensor was highly anisotropic with  $\langle 111 \rangle$  principal-axes. They indicate that the  $\text{Eu}^{2+}$  ions are probably nearest neighbors to oxygen vacancies. The  $\text{Eu}^{2+}$  ions bleach very slowly at room temperature and rapidly with uv illumination. The excitation and bleaching behavior are similar to those for the 149 °C retrapping states, but the EPR spectra are much different.

The most recent study is by Kolopus, Finch, and Abraham who observed various EPR spectra in thoria grown from  $\text{PbO-}$ ,  $\text{PbF}_2\text{-}$ , and  $\text{Li}_2\text{O} \cdot 2\text{WO}_3\text{-}$  based solvents after irradiation with  $^{60}\text{Co}$   $\gamma$  rays, 2-MeV electrons, or with neutrons.<sup>31</sup> The types and numbers of centers depended on the growth method and type of irradiations. No EPR spectra were observed in any of the crystals prior to irradiation. Irradiation of  $\text{PbO-}$  and  $\text{PbF}_2\text{-}$  grown crystals with electrons of  $\gamma$ 's at 300 °K produced resonances with  $g = 1.9666$ , which were identified as being due to  $\text{Pb}^{3+}$  ions in cubic sites; the  $\text{PbF}_2\text{-}$  grown crystals also had induced resonances with  $\langle 111 \rangle$  axes with  $g_{\parallel} = 1.9704$  and  $g_{\perp} = 1.9637$ , and these are attributed to  $\text{Pb}^{3+}\text{-F}^-$  complexes. Both kinds of centers have high-field hyperfine lines due to  $^{207}\text{Pb}^{3+}$ , and the spectrum for the axial center is split, into parts which they label A and B, by the interaction with the fluorine ion. Neutron irradiation at 300 °K produced (100) axial centers with  $g_{\parallel} = 1.812$  and  $g_{\perp} = 1.925$  in all crystals, but the number of centers was greatest in those grown with  $\text{Li}_2\text{O} \cdot 2\text{WO}_3$ . One  $\text{Li}_2\text{O} \cdot 2\text{WO}_3\text{-}$  grown crystal that was irradiated with neutrons at 130 °K was observed at 77 °K to have  $\langle 111 \rangle$  centers with  $g_{\parallel} = 2.003$  and  $g_{\perp} = 2.095$ , and the center annealed below 300 °K. Other weaker spectra were observed in some crystals after electrons and  $\gamma$  irradiation, but they were not studied.

Kolopus *et al.* noted that within experimental error the  $g$  tensor for the part of the  $\text{Pb}^{3+}\text{-F}^-$  EPR spectrum labeled A is the same as that which was observed by Neeley *et al.*, and they question the F-center interpretation since the crystals used in the earlier work were grown with fluxes containing  $\text{PbF}_2$ . The  $g$  values observed by Neeley, Neaves, and Kolopus and their co-workers are  $g_{\parallel} = 1.9739$ , 1.9742, and 1.9704 and

$g_1 = 1.9644$ ,  $1.9619$ , and  $1.9637$ . It could be that these  $g$  values are for different centers since there are unexplained differences. Neeley *et al.* observed only one line and it was narrower at  $4^\circ\text{K}$  than the corresponding line measured by Kolopus *et al.* Neaves and Tint measured only the two lines, which were much narrower at  $77^\circ\text{K}$ , and the  $\langle 100 \rangle$  splitting is only 11 G while that for axial  $\text{Pb}^{3+}\text{-F}^-$  is about 15 G. It is strange that Neeley *et al.* did not observe more of the lead spectra. It is also curious that Kolopus *et al.* did not observe any of the spectra discussed by Neaves and Tint since the crystals were from the same source and grown in the same  $\text{Li}_2\text{O}\cdot 2\text{WO}_3$  flux.

#### Association of Electronic Charge with Crystal Defects

TL and EPR measurements can be used to detect with good signal-to-noise ratio less than  $10^9$  transitions or  $10^{11}$  charges, respectively. This means characteristic responses can be observed for very small defect densities even for quite small specimens. This high sensitivity is advantageous when the characteristics are recognized; the difficulty is that the trapping states may be associated with unknown defects whose densities are too small to be measured by a general impurity analysis. In any case, correlations with defect densities is complicated because trapping states are not necessarily filled at saturation, and because the efficiency for TL for the trapped charges is usually unknown.

Twelve single crystals of thoria were analyzed for impurities by spark-source mass spectrographic analysis, and when possible, by optical emission analysis.<sup>2</sup> Many of the crystals had a volume of  $10^{-3}\text{ cm}^3$  or less so that accurate analysis was difficult. There were only a few elements that were present in more than one sample in appreciable quantities (a few ppm wt or more); there were very few elements present in large concentrations. The only impurities that were found in appreciable quantities in most samples were C, Na, Si, S, Cl, and Ce. Most of these elements are present in the highest concentrations in the samples that have weak-to-moderate TL. There is no indication that any of the elements except cerium either increase or decrease the optical activity. The only foreign atoms that are known to participate in the TL are the rare earths, and their role is not yet understood completely.

Lead and fluorine bear special consideration in view of the EPR observations of Kolopus *et al.*<sup>31</sup> The Perkin-Elmer crystals which were supplied by Linares contained about 100 ppm wt fluorine and 100–600 ppm wt of lead while all others studied contained less than 1 ppm wt of lead. Kolopus *et al.* suggest that the lead goes in  $\text{ThO}_2$  as  $\text{Pb}^{2+}$  and that the irradiation converts the lead

to  $\text{Pb}^{3+}$ . If this is correct, then the lead ions act as electron sources which compete with other electron sources to fill the available electron traps and in being available for recombination. This is consistent with the fact that the rare-earth TL intensity is reduced in the Perkin-Elmer crystals, if present at all. A study of the annealing behavior for the lead-associated EPR spectra should clarify whether the lead is initially in a divalent or quadravalent state.

In most cases, the conditions we used for observing TL were such that each unit of area in the plots used for dosage or excitation spectra studies corresponds to about  $10^{10}$  photons with a 550-nm wavelength being emitted from a crystal. For the  $\text{ThO}_2$  crystals used in this study, the number of visible photons emitted during a total glow curve at saturation varied from  $10^{14}$  to  $10^{18}$  per  $\text{cm}^3$  of crystal volume. For example, we estimate that the total number of visible TL transitions in OR2, volume  $0.0043\text{ cm}^3$ , at saturation is about  $4 \times 10^{13}$ , or about  $10^{16}/\text{cm}^3$ . Wagner *et al.* estimate from EPR that there are about  $3 \times 10^{13}$   $\text{Er}^{3+}$  ions and that the total number of observable spins created by irradiating OR2 to saturation is about  $10^{13}$ . The peak-by-peak correspondences of the number of transitions and trapped electrons are quite different, but still these numbers do provide a general indication that the number of emitted photons per trapped charge is not greatly different from unity for OR2.

It is clear from the impurity analyses, that a small amount of rare-earth ions can dominate the TL emission. The number of visible photons emitted at saturation per rare-earth ion was estimated in a number of cases. An erbium-doped crystal has about 10-ppm wt erbium, or about  $10^{15}$  erbium atoms in its  $10^{-3}\text{-cm}^3$  volume. The total area under the glow curve at saturation indicates, according to our calculations, that  $1.3 \times 10^{14}$  photons were emitted from the crystal. Therefore, one photon was emitted for every eight erbium ions. On the other hand, another undoped crystal OR7 contained only 0.07 ppm wt of erbium and it emitted approximately  $2 \times 10^{13}$  photons from its  $0.0033\text{-cm}^3$  volume, which led us to estimate that 240 photons were emitted for each 100 erbium ions. (We really do not believe that there was more than one photon per erbium ion and ascribe this result to errors in the estimate.) Similar calculations, which included appropriate photomultiplier response factors, indicated that after being excited to saturation, a crystal doped with 600 ppm wt of europium emitted one TL photon for every 20 europium ions, and that a crystal doped with 30 ppm wt of dysprosium emitted one photon for every 50 dysprosium ions. The rather high probability that thermal activation of a trapped

electron will result in trivalent-rare-earth emission in a weakly doped crystal like OR2 suggests that the rare-earth ions provide deep trapping states for holes which can capture thermally activated mobile electrons. It does not necessarily mean that the rare-earth ions change valence since nearby oxygen ions could capture the hole.

It may be that the major trapping state in the thoria crystals are associated with intrinsic crystal defects since the relative intensities of glow peaks show no major dependence on the variation in impurity levels in various crystals. The large changes in the number of trapped charges or emitted photons with rare-earth doping suggest that the rare earths do induce trapping defects which include oxygen vacancies as key ingredients. The shifts in peak temperatures with rare-earth dopant indicate that some of the trap activation energies may be sensitive to the rare-earth dopant. Thermal quenching temperatures are probably higher for the rare earths than for most luminescence activators, and this can mean that the rare-earth ions are essential to the observation of thermal activation of charge from the deeper traps by TL.

#### DISCUSSION OF MODELS

The foregoing observations of cyclic photoelectronic processes in thoria provide a lot of detailed conditions that must be consistent with any interpretations in terms of models. Some of the most important factors we have to consider are the following: (a) The peaks in TL excitation efficiency and in the absorption for undoped thoria crystals both occur at about 210 nm; this implies that the excitation process is dominated by transitions from the  $O^{2-}$  to the  $Th^{3+}$  band. This process provides mobile electrons and holes which can be trapped at or near suitable defects. (b) The TL is dominated by the characteristic emission from the trivalent states of rare-earth ions when they are present; we have indicated earlier that oxygen ions in the neighborhood of rare-earth ions in cubic sites may capture some of the mobile holes and that the TL results because energy is transferred to the rare-earth ions when the thermally activated mobile electrons recombine with the rare-earth-associated trapped holes. The thermal annealing of EPR lines revealed the thermal activation of hole states at about  $-127$  and  $151$  °C. The fate of the holes activated at  $-127$  °C is unknown. The holes which are activated at  $151$  °C are primarily captured by the remaining trapped electrons rather than being re-trapped by the deep hole traps which are associated with rare-earth ions. (c) The detailed results of the TL and EPR studies of electron traps provides information about activation energies, frequency factors, retrapping, bleaching,  $g$  shift and  $g$  symmetry. (d) The EPR measurements showed that all of

the trapped electrons are subjected to local crystal fields having  $C_{3v}$  symmetry; and there were no indications of hyperfine structure resulting from nuclear moments. (e) The TL glow curves from many crystals from different sources are similar to the extent that the properties appear to be intrinsic, and this suggests that oxygen vacancies may be essential to the formation of some of the trapped electron states. If single vacancies are involved, then the Jahn-Teller effect would explain the reduction from  $T_d$  to  $C_{3v}$  symmetry.

Some effects on optical properties resulting from attempts to induce oxygen vacancies have been reported by Weinreich and Danforth,<sup>13</sup> Danforth,<sup>32</sup> Linares,<sup>8</sup> and Bates.<sup>20</sup> The most directly related earlier work is that by Neeley, Gruber, and Gray who observed one relatively broad x-ray-induced and infrared bleachable EPR line corresponding to the resonances for retraps A.<sup>29</sup> Neeley *et al.* argued that the line is probably associated with singly charged oxygen vacancies because they observed that the EPR line strength varied with erbium and lanthanum doping levels which they noted should have induced oxygen vacancies for charge compensation. We have also observed an increase in TL intensity with rare-earth doping. The absence of hyperfine structure does suggest that the rare-earth ions are not directly involved in forming the electron-trapping states, but to insure this, it would be desirable to vary the oxygen-vacancy concentration by other methods, as by  $\gamma$ -ray damage, or by quenching crystals from reduced equilibrium conditions, or by doping with other elements that would require oxygen-vacancy charge compensation. Furthermore, consideration must be given to the fact that a variation of trapping defect densities can correlate directly with the number of trapped charges only if there is an excess of charge sources or of traps for charges of the opposite sign.

In his thesis, Rodine considered the possibility that an electron might be trapped at various energy levels by a single oxygen vacancy. This idea was advanced in an attempt to account for the retrapping by the electron traps which anneal near  $150$  °C and for the failure to achieve direct excitation of these traps with uv light at  $77$  °K. Thus, it was proposed that electron capture by individual thorium ions from the successive shells neighboring a vacancy might account for the apparently intrinsic glow peaks near  $-103$ ,  $-14$ , and  $149$  °C. It was suggested that the shallower states could shield the deeper states during the excitation, and that the deeper states would compete for the charge released when the shallower states were thermally activated. As pointed out in the thesis, this model

does not account for the absence of EPR lines for the  $-103$  and  $-14$  °C glow peaks, nor does it account for the selective uv bleaching of the  $149$  °C traps and the related fact that these traps cannot be populated appreciably with uv light at  $20$  °C. There are various other objections to this kind of model. First of all, the simple vacancy model does not provide an explanation for the different, but very similar  $g$  values for the isoenergetic  $149$  °C traps. Secondly, the  $-103$ ,  $-14$ , and  $149$  °C glow peaks saturate at different dose levels in some crystals, and the relative amounts of glow at saturation change from crystal to crystal. For example, in some crystals, the peak near  $149$  °C becomes dominant after the other peaks have saturated. This is most apparent from recently obtained dosage curves for an europium-doped crystal. Thirdly, a basic difference in glow-peak sources is indicated by the fact that the growth with dose for the  $-14$  °C peak is always linear or sublinear; while at low dose, the growth of the  $-103$  and  $149$  °C peaks is quadratic.

In the course of attempting to explain the absence of EPR lines for the  $-103$  and  $-14$  °C traps, Rodine also considered the possibility that for OR2 the  $-158$ ,  $-103$ , and  $150$  °C glow peaks might result from changes in valence of a single defect. Thus, one might suppose that the  $-158$  °C peak results from thermal activation of trivalent oxygen vacancies ( $F^{\cdot}$  centers) while the  $-103$  and  $149$  °C peaks result from divalent vacancies ( $F$  centers) and monovalent vacancies ( $F^+$  centers), respectively. Models of this kind suffer all of the shortcomings of the previous model and furthermore, it is not reasonable that the states having the smallest observed metastable valence would not be created directly by the uv excitation that forms the states of higher valence.

In his thesis, Tint proposed defect models to account for all of the EPR lines that he and Neaves observed.<sup>4</sup> He estimated or calculated energy levels for some models by the method of Pincherle,<sup>33</sup> and by the more accurate and involved methods of Gourary and Adrian.<sup>34,35</sup> The magnitudes and anisotropy of  $g$  shifts were estimated for some models by the methods which have been used by Kahn and Kittel,<sup>36</sup> and by Blumberg and Das,<sup>37</sup> respectively. We are not familiar with all of these analyses, and we have not attempted to follow the rather involved calculations in detail. Certainly, the approach taken by Tint is essential, and even if some of the models for traps are inappropriate, his calculations, estimates, and discussion should be generally useful to the study of thoria and similar crystals.

The model Tint proposed for the  $-158$  °C trap was the  $F^{\cdot}$  center. This was considered appropriate on the basis of energy without making specific

estimates which would have been quite difficult, on the basis of the symmetry which was originally thought to be isotropic, on the basis of the need for an odd number of electrons, and on the basis that no hyperfine structure was observed. Subsequent measurements<sup>5</sup> have detected a slight asymmetry which could possibly be accounted for by the Jahn-Teller effect.

Tint proposed that two changes in valence of a single defect might account for the  $-103$  and  $149$  °C glow peaks, but we have shown in a previous paragraph that this kind of model is inconsistent with several facts. He considers a basic defect which consists of a vacant thorium site with two nearest-neighbor oxygen vacancies such that all of the vacancies occur on a  $\langle 111 \rangle$  axis. This defect is neutral, and it would seem reasonable that it could provide a shallow electron or hole trap, or possibly a localized trapped electron-hole pair. Tint however, develops the basic model further by adding two electrons at each of the oxygen vacancies, and one  $O^{\cdot}$  ion at one of the interstitial sites which are off and on the basic defect symmetry axis in a ratio of 3:1. Loss of one of the electrons at  $-103$  °C is considered to convert the defects to the states having the two retrap resonances  $A$  and  $B$  which for OR2 are observed with a 3:1 absorption ratio. Tint argues that the off-diagonal  $O^{\cdot}$  interstitials may not lower the symmetry appreciably; this may be plausible, but the six units of charge in the model, which are imposed by the method of calculation, appear to be excessive.

The trapping model proposed to account for the  $174$  °C glow peak is an electron in an oxygen vacancy with an  $O^{\cdot}$  ion replacing one of the nearest-neighbor  $Th^{4+}$  ions and an  $O^{\cdot}$  ion in one of the normally empty nearest-neighbor cubic sites. The vacancy and extra oxygen ions are on a  $\langle 111 \rangle$  axis. The model has an excess negative charge of seven electron units which does not seem realistic.

Tint also discussed the possibility that the EPR lines for hole traps are due to  $V_F$  and  $V_K$  centers. The  $V_K$ , or self-trapped hole center, seems to be a reasonable candidate to explain the electron resonance that anneals at  $-127$  °C since this is the least tightly bound hole observed. The  $V_F$  center, which is described as a hole trapped next to a  $Th^{4+}$  vacancy, would probably have a binding energy greater than  $1.5$  eV, whereas a reasonable estimate of the thermal activation energy for the  $150$  °C hole would be less than  $1.5$  eV.

The electron states we observed have activation energies in the range  $0.2$ – $1.5$  eV. If we neglect the anisotropy and treat the crystal as a continuum, then a simple central-field approximation yields hydrogenlike states with a ground-state energy

$$E(\text{eV}) = E_h Z^2 m^* / K^2 m_e = -0.63 Z^2 m^* / m_e, \quad (1)$$

where  $E_h = -13.57$  is the ground-state energy for a hydrogen atom,  $Z$  is the charge,  $m^*$  is the effective mass which is unknown,  $K = 4.63$  is the high-frequency dielectric constant, and  $m_e$  is the mass of a free electron. The ground-state radius is given by

$$r(\text{\AA}) = a_0 K m_e / m^* Z = 2.45 m_e / m^* Z, \quad (2)$$

where  $a_0 = 0.529 \text{\AA}$  is the radius for the ground state of a hydrogen atom. If one takes  $Z = 1$  and  $m^* = m_e$ , then  $r$  is very close to the nearest-neighbor distance  $r_0 = 2.425 \text{\AA}$ . This "continuum" model does not apply at this distance; the calculated values for  $E$  and  $r$  should be increased by decreasing  $K$  in order to compensate for the decrease from the assumed amount of shielding, but this change might be partially compensated by the effect of a corresponding increase in the effective mass. The central field approximation also gives

$$E(\text{eV}) = -7.2Z/\text{Kr}(\text{\AA}) = -1.55Z/r(\text{\AA}), \quad (3)$$

which indicates that the radii for  $Z = 1$  for the major electron traps in OR2 are as given by Table IV. These radii are too small for the approximation to be valid and they should be increased by appropriate decreases in the values for  $K$ . The radii double for  $Z = 2$ .

On the basis of the above model, doubly charged defects are less attractive candidates than singly charged defects because the energy estimated from Eq. (1) is much larger than the observed activation energies. For example, taking  $Z = 2$ ,  $K = 2$ , and  $m^* = m_e$  yields  $E = -13.57 \text{ eV}$  and decreasing  $K$  to unity yields  $E = -54.28 \text{ eV}$ . These energy estimates, which apply to the  $F^+$  center, are too large because they are larger than the band-gap energy of  $5.75 \text{ eV}$ . The energies for those tight-binding calculations which have been made are also too large. Tint calculated an energy of  $-41 \text{ eV}$  for the  $F^+$  center by a method of Gourary and Adrian. He used an  $s$ -type wave function and the Madlung potential for an unrelaxed crystal lattice. The energy estimates for the loose-binding or continuum model might be improved by decreasing  $Z$  from 2 to account for lattice relaxation, but there is obviously a need for tight-binding calculations that combine  $\text{Th}^{3+}$  orbitals to form wave functions which satisfy  $T_d$  of  $C_{3v}$  symmetry and that employ one or more lattice-relaxation parameters.

We will now review again the major properties observed for the electron traps and the models considered. All resonances occurred at sites having  $C_{3v}$  symmetry. This symmetry could occur by removal or by replacement of an oxygen atom if the normal  $T_d$  symmetry was reduced by the appropriate Jahn-Teller distortion,<sup>38</sup> but we do not know of any analogous cases where this occurs.

The  $C_{3v}$  symmetry occurs naturally for oxygen divacancies or for any defect complex whose components are joined by a  $\langle 111 \rangle$  axis, as for example, an oxygen vacancy and a rare-earth ion on a nearest-neighbor thorium site, or an interstitial rare earth with two other rare-earth ions on neighboring thorium ion sites. The simple vacancies, interstitials or complexes formed from vacancies and interstitials are attractive models for consideration because the major traps appear to be intrinsic to the host crystal, and because there is no observed splitting of the EPR lines by nuclear moments.

The wave functions for oxygen vacancies or for shallow electron states in thoria should be formed from a linear combination of  $\text{Th}^{3+}$  orbitals. There is a possibility, as was mentioned before, that a trapped electron may be associated with a single thorium ion in some shell neighboring a defect, but this possibility is excluded for the states which are observed by EPR for all except the first neighbor ions, because a random distribution over more distant ions would result in some nonaxial  $g$  tensors.

The above discussion of ground-state binding energies and radii indicates that the  $149^\circ\text{C}$  trapped electrons are very probably within the nearest-neighbor distance to the defect center so that the absence of hyperfine EPR structure, in addition to the indications of omnipresence, is a strong indication of an intrinsic defect. The  $F^+$  center must remain a candidate in spite of the unfavorable indications of binding energy calculations because it has an unpaired electron, but because of symmetry considerations the  $M^+$  center or trivalent divacancy may be a better candidate. The omnipresence of major glow peaks in the neighborhood of  $-100$  to  $-135^\circ\text{C}$  might be explained as being characteristic of the thoria crystal with singly charged defects that could include impurities. The shallower traps have less likelihood of hyperfine EPR structure and the shift in peak temperature with different defects could be explained with the continuum model by adjusting the  $Z$  value to account for an appropriate lattice relaxation.

#### SUMMARY

In summary, we will list some of the more important observations and conclusions resulting

TABLE IV. Radii for  $Z = 1$  for the major electron traps in OR2.

$T(^{\circ}\text{C})$	149	-14	-103	-158
$E(\text{eV})$	-1.37	-0.83	-0.46	-0.28
$r(\text{\AA})$	1.13	1.86	3.33	5.63
$r/r_0$	0.46	0.77	1.37	2.32

from this work:

1. The glow curves are very similar to each other; this is especially true for crystals which have a TL that is characteristic of trivalent rare-earth ions, but it also holds for relatively impure crystals which have a TL emission of unknown origin. The fluorescence of the impure crystals could be a mixture of rare-earth lines.

2. The largest TL peaks after uv or x-ray excitation at 77 °K have maxima near -160, -130 to -100, -14, and 130-160 °C.

3. The visible fluorescence and TL emission of the batch of high-purity thoria crystals which yielded OR2 was dominated by erbium which was present at approximately  $3 \times 10^{-7}$  Er/Th. The TL is fairly bright green to the eye when the crystals are warmed in 20 °C air from 77 °K, even for this low doping level. The fluorescence is not very bright at the excitation levels which we used, and at 77 °C, the emission from most crystals of the batch were due to trace  $Gd^{3+}$ .

4. The fluorescence emission appears to be the same as the TL at the same temperature in the rare-earth dominated crystals.

5. The EPR spectra for the  $Er^{3+}$  and  $Gd^{3+}$  in cubic sites decay with uv irradiation at 77 °K. For TL saturation conditions, no x-ray induced fluorescence spectra are observed which might be associated with direct excitation of divalent or quadrivalent rare-earth ions. There were no gross changes in the fluorescence of OR2 when it was excited to saturation with uv, but the fluorescence was too weak for this to be a definite indication that the holes are on the neighboring oxygens.

6. The dosage curves for several peaks -160, -103, 80, and 150 °C, indicate initial growth that is usually quadratic with time. This is explained by the fact that deep electron traps compete with the luminescence-active holes for the thermally released electrons. Thus, the TL increases initially as the product of the occupation numbers of the electron traps and luminescence hole traps which individually grow linearly with time. The total TL is linear with dose since all of the luminescent hole states recombine radiatively with mobile electrons.

7. The dosage curves indicate that the TL peaks near -180 and -14 °C tend to have large regions of sublinear growth with time. The 174 and 220 °C peaks tend to have linear growth with time since there is no large number of deeper electron traps to compete with hole recombination processes.

8. In many cases, the dosage curves indicate a tendency for TL peaks to reach saturation at about the same time, and this indicates saturation of hole traps. In some cases, some TL peaks do saturate at intermediate dose levels which indicates

that the associated electron traps reach maximum occupation before the hole traps are substantially filled. This is most usual for the peak near -14 °C which also tends to have a sublinear growth and dominance of the glow at very low dose, but it also occurs for the less prominent peaks near -90, -53, and 80 °C.

9. The four EPR dosage curves for electron and hole traps in OR2 showed something less than two decades of approximately linear growth with dose which corresponds to the upper part of the TL dosage curves. The growth is linear since the EPR absorptions are proportional to the trap occupation numbers. The EPR spectra corresponding to the 150 °C hole reached a maximum and then decayed by about a factor of 0.1, and this is an indication that the electron traps in OR2 are filled before the hole traps are filled.

10. The EPR measurements indicate that the numbers of electrons observed in different traps in OR2 fall within an order of magnitude of each other, whereas the TL shows that the glow maxima from the peaks near -103 and 150 °C at saturation are approximately 25 times larger than that from the peaks near -158 and 174 °C. The difference is attributed to strong retrapping by deeper traps while heating through the -158 °C region, and to recombination of thermally activated holes with the 174 °C trapped electrons, when heating through the 150 °C temperature range. The thermal activation of 150 °C holes also causes truncation of the 149 °C glow peaks in OR2. Some truncation is usually observed for peaks in this range and the most prominent case is for a peak at about 135 °C for a europium-doped crystal.

11. Excitation of the TL due to the radioactivity of thorium was observed in N1, which was one of the larger crystals. The rate of self-excitation is much smaller than the rate of excitation by the uv radiation used in this work, so it is not an important factor except in the cases of very low dose.

12. The traps responsible for the 149 °C TL peak cannot be populated to an appreciable extent by uv irradiation at room temperature; the EPR study of OR2 indicated that the associated traps are bleached by uv irradiation at 77 °K and that the bleaching probability for traps increases with decreasing occupation number; subsequent TL studies showed that the traps are bleached by all wavelengths above 215 nm at 300 °K. This is in contrast to what one could expect from a study by Finch *et al.* which we referred to earlier. Excitation with x rays does fill the 149 °C electron traps and other deep electron traps directly and this is in accord with the observations of x-ray-induced EPR spectra that is stable at room temperature. The uv bleaching behavior is like the behavior of the divalent europium-oxygen vacancy complex ob-

served by Kolopus *et al.*, but the EPR spectra are quite different.

13. A band gap for thoria of 5.75 eV is indicated by the peak in TL excitation at 210 nm for the undoped Oak Ridge thoria and by the edge in absorption which occurred at or near 215 nm.

14. The traps in the undoped thoria from Oak Ridge are populated most readily by the 210-nm band-gap excitation, but there are indications of preferential excitation of some traps by some wavelengths both above and below 210 nm. The TL excitation maximum for a europium doped crystal, OR2, was at 220 nm and there was no indication of a maximum near 260 nm where the maximum for fluorescence excitation occurs.

15. Evidence for self-retrapping was observed for the  $-14$  and  $-103$  °C peaks by the decrease of peak temperature with increasing dose; the shifts could, of course, be a result of peak multiplicity.

16. The charge in the traps which give rise to TL can be optically bleached by a broad band of IR, visible, and uv light. The onset of bleaching is not sharp so there are no well-defined optical activation energies. Some of the charges which are optically activated from shallow traps are re-trapped by deeper traps.

17. The correspondence between TL and EPR of OR2 indicates that thermal activation of electrons at  $-158$  °C may result in strong retrapping by the  $-103$  and perhaps the  $-14$  °C trap; it definitely shows that part of the charge released during the  $-103$  and  $-14$  °C TL peaks is retrapped by the  $150$  °C traps and in proportion to the relative TL intensity of the  $-103$  and  $-14$  °C peaks.

18. The thermal activation energy and frequency factor analyses by three methods showed good agreement between crystals and variations among methods of analysis. The differences between methods is considered to be a consequence of peak

multiplicity and self-retrapping. The thermal activation energies had values such as 0.2 eV for the  $-160$  °C peak and 1.25 eV for the  $150$  °C peak. It is believed that the initial-rise analysis yielded the most appropriate energy values.

19. The EPR lines associated with the  $150$  °C TL peak appear to have the same  $g$  tensor as measured in a previous investigation in which the line was attributed to a singly charged oxygen vacancy.<sup>29</sup> We also believe on the basis of similarity of glow curves, the variation of total TL with rare-earth doping level, and the site symmetry of the electron traps that oxygen vacancies are essential to the principal trapping defects, but they may be complexed.

#### ACKNOWLEDGMENTS

The authors are indebted to Dr. Cabell Finch and Dr. G. Wayne Clark of the Oak Ridge National Laboratories for generously providing many of the ThO<sub>2</sub> crystals, some of which were grown in response to our specific requests, and for permission to use unpublished data. We wish to thank Dr. A. Neaves and Dr. G. S. Tint of the Franklin Institute for their fine cooperation which made their work and ours mutually beneficial. We also thank Dr. G. Wagner, Dr. D. Feldman, and Dr. J. Murphy of Westinghouse Research Laboratories for their continuing efforts with regard to the resonance studies of these crystals, for helpful discussions, and for furnishing unpublished data. Thanks are due to Dr. R. C. Linares for supplying some of the ThO<sub>2</sub> crystals. We also wish to thank Professor John W. Weymouth of the University of Nebraska for useful and stimulating discussions during the course of this work. Finally, we wish to express our thanks to Mr. E. J. Hassell and Dr. N. M. Tallan, who directed the laboratory research program for the study of defects in ionic materials.

\*Work partially supported under contract by Aerospace Research Laboratories, Wright-Patterson AFB, Ohio 45433.

<sup>1</sup>E. T. Rodine, Ph.D. thesis (University of Nebraska, 1970) (unpublished).

<sup>2</sup>E. T. Rodine, Aerospace Research Laboratories Technical Report No. ARL 70-0138, 1970 (unpublished).

<sup>3</sup>A. Neaves and G. S. Tint, Aerospace Research Laboratories Technical Report No. ARL 69-0071, 1969 (unpublished).

<sup>4</sup>G. S. Tint, Ph.D. thesis (Temple University, Philadelphia, Pa., 1970) (unpublished).

<sup>5</sup>G. R. Wagner, D. W. Feldman, and J. Murphy, United States Air Force Summary Report Contract No. F33615-68-C-1681, 1970 (unpublished); and subsequent reports.

<sup>6</sup>E. H. Greener, W. M. Hirthe, and E. Angino, Jr., Chem. Phys. **36**, 1105 (1962).

<sup>7</sup>C. B. Finch, L. J. Nugent, G. K. Werner, and M. M. Abraham, in Seventh Rare-Earth Research Conference, San Diego, Calif., 1968 (unpublished).

<sup>8</sup>R. C. Linares, J. Phys. Chem. Solids **28**, 1285 (1967).

<sup>9</sup>P. L. Land and E. D. Wysong, in Proceedings of the Second International Conference on Luminescence Dosimetry, Gatlinburg, Tenn., 1968, Oak Ridge National Laboratory Division of Technical Information Conference No. 680920 (unpublished).

<sup>10</sup>P. L. Land and E. T. Rodine, Aerospace Research Laboratories Technical Report, 1971 (unpublished).

<sup>11</sup>P. L. Land, J. Phys. Chem. Solids **30**, 1681 (1969).

<sup>12</sup>C. B. Finch and G. Wayne Clark, J. Appl. Phys. **36**, 2143 (1965).

<sup>13</sup>O. A. Weinreich and W. E. Danforth, Phys. Rev. **88**, 953 (1952).

<sup>14</sup>P. L. Land, J. Phys. Chem. Solids **30**, 1693 (1969).

<sup>15</sup>A. Halperin and R. Chen, Phys. Rev. **148**, 839 (1966).

See also N. Kristianpoller and M. Israeli, *Phys. Rev. B* **2**, 2175 (1970).

<sup>16</sup>R. C. Linares, *J. Opt. Soc. Am.* **56**, 1700 (1966).

<sup>17</sup>A. K. Trofimov, *Izv. Akad. Nauk. S. S. S. R., Ser. Fiz.* **25**, 460 (1961).

<sup>18</sup>M. J. Weber, *Phys. Rev.* **171**, 283 (1968).

<sup>19</sup>J. L. Merz and P. S. Pershan, *Phys. Rev.* **162**, 217 (1967).

<sup>20</sup>J. L. Bates, AEC Report No. BNWL-457, 1957 (unpublished).

<sup>21</sup>M. H. L. Price, *Proc. Phys. Soc. (London)* **A63**, 25 (1950).

<sup>22</sup>M. H. L. Price, *Nuovo Cimento Suppl.* **6**, 817 (1957).

<sup>23</sup>T. G. Castner and W. Kanzig, *J. Phys. Chem. Solids* **3**, 178 (1957).

<sup>24</sup>S. A. Al'tshuler and B. M. Kozyrev, *Electron Paramagnetic Resonance* (Academic, New York, 1964), Secs. 3.3 and 6.5.

<sup>25</sup>C. P. Slichter, *Principles of Magnetic Resonance* (Harper and Row, New York, 1963), Secs. 7.2 and 7.4.

<sup>26</sup>W. Low and D. Shaltiel, *J. Phys. Chem. Solids* **6**, 315 (1958).

<sup>27</sup>M. Abraham, R. A. Weeks, G. W. Clark, and C. B. Finch, *Phys. Rev.* **137**, A138 (1965).

<sup>28</sup>M. M. Abraham, E. J. Lee, and R. A. Weeks, *J. Phys. Chem. Solids* **26**, 1249 (1965).

<sup>29</sup>V. I. Neeley, J. B. Greber, and W. J. Gray, *Phys. Rev.* **158**, 809 (1967).

<sup>30</sup>M. M. Abraham, C. B. Finch, R. W. Reynolds, and H. Zeldes, *Phys. Rev.* **187**, 451 (1969).

<sup>31</sup>J. L. Kolopus, C. B. Finch, and M. M. Abraham, *Phys. Rev. B* **2**, 2040 (1970).

<sup>32</sup>W. E. Danforth, *Advances in Electronics*, Vol. 5 (Academic, New York, 1953).

<sup>33</sup>L. Pincherle, *Proc. Phys. Soc. (London)* **A64**, 648 (1951).

<sup>34</sup>B. S. Gourary and F. S. Adrian, *Phys. Rev.* **105**, 215 (1957).

<sup>35</sup>B. S. Gourary and F. S. Adrian, *Solid State Physics*, Vol. 10 (Academic, New York, 1960).

<sup>36</sup>A. H. Kahn and C. Kittel, *Phys. Rev.* **89**, 315 (1953).

<sup>37</sup>W. E. Blumberg and T. P. Das, *Phys. Rev.* **110**, 647 (1958).

<sup>38</sup>F. S. Ham, *Phys. Rev.* **166**, 307 (1968).

PHYSICAL REVIEW B

VOLUME 4, NUMBER 8

15 OCTOBER 1971

## Direct Observation of Isolated $J=1$ Pairs in Solid Deuterium and Hydrogen by Raman Scattering

Isaac F. Silvera\* and Walter N. Hardy†

*North American Rockwell Science Center, Thousand Oaks, California 91360*

and

John P. McTague

*Department of Chemistry, University of California, † Los Angeles, California 90024*

(Received 1 March 1971)

Spectra due to the orientational states of isolated  $J=1$  impurity pairs in solid hydrogen and deuterium have been observed by Raman scattering in the wave-number range  $2.3\text{--}7\text{ cm}^{-1}$ . The results give a direct measure of the pair energy levels and can be used to determine the anisotropic pair interactions. To within experimental accuracy, no deviation from the dominant electric quadrupole-quadrupole interaction was observed. Expressions are developed for the scattering efficiency which agree well with experiment. Zero-point-motion averages of the interactions are calculated using several quantum crystal wave functions and a comparison is made with the measured frequencies. The collective wave functions give better agreement with experiment than the Hartree single-particle wave functions.

### I. INTRODUCTION

The solid hydrogens (hydrogen, hydrogen deuteride, and deuterium) are the simplest molecular solids and present unique opportunities for the study of intermolecular interactions in the crystal-line state. Their interactions with electromagnetic radiation provide rich spectra that can be interpreted in terms of intermolecular forces; the variation of mass by a factor of 2 with little change in the electronic structure enables studies of mass effects; and the anisotropic interactions can be isolated by studying appropriate mixtures of the ortho-para species. In the condensed phase the hydrogens, as distinct from most solids, exhibit well-resolved

rotational spectra. This is a consequence of the fact that the free-molecule rotational energy spacings are much larger than the anisotropic potentials in the solid, and thus the rotational quantum number  $J$  remains a good quantum number.

At the low temperatures of the solid ( $< 20\text{ K}$ ) essentially all hydrogen (deuterium) molecules are in the lowest accessible rotational level, namely,  $J=0$  for para-hydrogen ( $p\text{-H}_2$ ) and ortho-deuterium ( $o\text{-D}_2$ ), and  $J=1$  for ortho-hydrogen ( $o\text{-H}_2$ ) and para-deuterium ( $p\text{-D}_2$ ). For low concentrations of  $J=1$  molecules the lattice structure is hexagonal close packed (hcp). Molecules in the  $J=0$  state interact only isotropically, while isolated  $J=1$  molecules experience very weak anisotropic interac-